

000 001 002 003 004 005 006 007 008 009 010 011 012 013 014 015 016 017 018 019 020 021 022 023 024 025 026 027 028 029 030 031 032 033 034 035 036 037 038 039 040 041 042 043 044 045 046 047 048 049 050 051 052 053 MULTIVERSE MECHANICA: A TESTBED FOR LEARN- ING GAME MECHANICS VIA COUNTERFACTUAL WORLDS

Anonymous authors

Paper under double-blind review

ABSTRACT

We study how generative world models trained on video games can go beyond mere reproduction of gameplay visuals to learning *game mechanics*—the modular rules that causally govern gameplay. We introduce a formalization of the concept of game mechanics that operationalizes mechanic-learning as a *causal counterfactual inference* task and uses the *causal consistency principle* to address the challenge of generating gameplay with world models that do not violate game rules. We present **Multiverse Mechanica**, a playable video game testbed that implements a set of ground truth game mechanics based on our causal formalism. The game natively emits training data, where each training example is paired with a set of causal DAGs that encode causality, consistency, and counterfactual dependence specific to the mechanic that is in play—these provide additional artifacts that could be leveraged in mechanic-learning experiments. We provide a proof-of-concept that demonstrates fine-tuning a pre-trained model that targets mechanic learning. Multiverse Mechanica is a testbed that provides a reproducible, low-cost path for studying and comparing methods that aim to learn game mechanics—not just pixels.

1 INTRODUCTION

Interactive world models have recently gained attention for their potential to simulate or extend video game experiences (Bruce et al., 2024; Parker-Holder & Fruchter, 2025; Decart et al., 2024; He et al., 2025; Che et al., 2025). SOTA models, typically leveraging deep autoregressive transformer architectures, are trained on large datasets containing sequences of visual frames, user inputs, or internal virtual states produced by a graphics engine. These models of video games (game world models) can generate gameplay sequences that are visually similar to original gameplay; an impressive feat considering modern video games often have cinematic levels of visual complexity.

A key motivation for a focus on video games is procedural generation of novel gameplay experiences (Gingerson et al., 2024). To this end, the ability to produce high-fidelity visuals is a necessity, as the novel experiences must look the part. But in addition to looking good, the game world model must generate gameplay that is **consistent** with the game’s **mechanics** (Gingerson et al., 2024). In simple terms, if the generated gameplay violates game rules or logic, it breaks the gaming experience and, therefore, is not useful, regardless of how good it looks.

Authors of game world models often claim to have learned a game’s *mechanics*—rules governing gameplay—through post-hoc observations of generated gameplay from the trained model, which visually demonstrates the mechanics in play. For example, in reference to their *World Models* framework, the authors Ha & Schmidhuber (2018) claim that “by learning only from raw image data collected from random episodes, [their model] learns how to simulate the essential aspects of the game, such as the game logic, enemy behavior, physics ...”. Kim et al. (2020) claim their *GameGAN* model learned the collision and power pellet mechanics of PAC-MAN. Parker-Holder & Fruchter (2025) claimed that consistency was an “emergent” property of Genie 3.

There is a problem with such claims. An *a posteriori* observation that a game world model has learned a mechanic demonstrates that it is *possible* to learn *some* mechanics in *some* contexts with SOTA architectures. However, this does not tell us *a priori* that it is possible to reliably reproduce

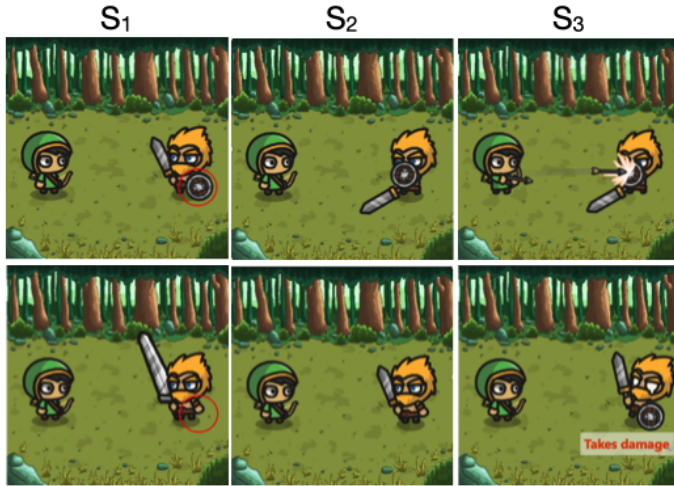


Figure 1: Clips from consistent contrasts sampled at their respective impact frames: each column contains two contrasting gameplay clips where differences are solely attributable to the shield mechanic. Left, middle, and right correspond to parallel world statements S_1 , S_2 , S_3 .

a certain context. To use a game world model to generate novel gameplay experiences in practical settings, we need this knowledge before expending on training and deploying a model.

Part of the difficulty is a lack of any formalized notion of what it means to learn a game mechanic. With a formal definition, we could determine if a mechanic is statistically identifiable from training data, and we could evaluate claims that a model has learned a mechanic. Moreover, we could define exactly what it is that we want to identify. The model needs to learn a representation of a mechanic sufficient to reliably reproduce it in generated gameplay, without going as far as reverse-engineering the mechanic’s source code; a formal definition would tell us the level of detail required. Lacking this, we cannot know when we have disentangled the mechanic’s representation from learning other representations that drive the game’s visuals.

In this paper, we address this problem with the following contributions. Firstly, we provide a **causal formalization** of the concept of game mechanics using causal graphical modeling theory. We use this formalization to demonstrate data and inductive biases (in the form of causal graphs) that enable learning a game mechanic. We introduce Multiverse Mechanica, a playable game for use as a testbed for evaluating the learning of game mechanics. The game mechanics are implemented with our causal graphical formalization, providing a ground truth for evaluating mechanic learning. It provides causal graphical representations of the mechanic directly to the user for use in evaluation or to supervise mechanic-learning. Multiverse Mechanica is visually simple enough to facilitate inexpensive experimentation, while it enables generalization by using mechanics that are typical of fantasy combat games. Finally, we provide a proof-of-concept for fine-tuning a generative model on a specific game mechanism that leverages these causal representations in its objective function.

2 BACKGROUND AND RELATED WORK

Defining Game Mechanics. Building on prior definitions (Lo et al., 2021), we define a *game mechanic* as a modular subset (Björk & Holopainen, 2004; Schaul, 2013; Thielscher, 2011; Zook & Riedl, 2019) of the *game rules* triggered by specific player/agent interactions (Lundgren & Bjork, 2003; Fullerton et al., 2004), producing changes in *game state* (Järvinen, 2008; Fabricatore, 2007) that shape gameplay visuals (Hunicke et al., 2004). These subsets entail causal relations with pre-conditions and effects, representable as logic, finite-state machines, behavior trees, or transition functions (Zook & Riedl, 2014; Thielscher, 2011; Schaul, 2013; Dormans, 2012; Zook & Riedl, 2019). We formalize this definition in Section 3.2.

Causal Framing. We adopt the *causal hierarchy*, which describes three levels of statements that employ causal logic: (level-1) observation, (level-2) intervention, and (level-3) counterfactual

108 109 110 111 112 113 114 115	116 117 118 119 120 121 122 123 124 125 126 127 128 129 130 131	132 133 134 135 136 137 138 139 140 141 142 143 144 145 146 147 148 149 150 151 152 153 154 155 156 157 158 159 160 161
Level	Statement	
1) Observation	“The scene <i>might</i> generate to show an enemy taking damage from an attack.”	
2) Intervention	“ <i>If</i> an enemy were given a shield and they blocked an incoming attack, <i>then</i> the scene <i>would</i> generate to show the enemy not taking damage.”	
3) Counterfactual	“ <i>Given</i> an enemy did not have a shield and the scene generated showing them taking damage from an incoming attack, <i>if</i> they instead had a shield and they blocked, the scene <i>would have</i> generated to show the enemy not taking damage.”	

Table 1: Examples of the three causal hierarchy levels, in the context of game scene generation.

(Bareinboim et al., 2022). A predictive statement, such as “The scene would generate in *this way*,” is a level-1 observational statement that asks questions about the distribution of possible game scene generations $P(\mathbf{V})$. A level-2 interventional statement targets outcomes under hypothetical interventions, such as “If an enemy were placed here (e.g., in a place it would not naturally appear), then the scene would generate in *this way*,”, asks questions about $P(\mathbf{V} \mid \text{do}(X=x))$. A level-3 counterfactual statement considers observed outcomes and how those outcomes might have been different under hypothetical interventions, and asks questions about joint outcomes under conflicting interventions, e.g., $(Y_{X=x}, Y_{X=x'})$ Consequently, Level-3 quantities encode “all-else-equal” comparisons across worlds. For example: “Given there was no enemy and the scene generated that way, if an enemy were placed here, the scene would generate in *this way*.” Table 1 provides examples of the three levels of statements, grounded in the context of video game scene generation. Further background on the causal hierarchy is provided in Appendix D.1.

We use causal DAGs and *structural causal models* (SCMs) (Pearl, 2009) to model mechanics as mechanisms (rules) (Bongers et al., 2018). For focusing on a mechanic’s variables, we reference *marginalized DAGs* (mDAGs) that preserve causal and interventional semantics while marginalizing others (Evans, 2016). The *causal consistency principle* states that variables not downstream of an intervention retain the same value across worlds (Pearl, 2010; Shpitser & Pearl, 2012); *counterfactual graphs* capture this cross-world consistency compactly (single nodes for shared variables; world-indexed nodes for affected ones) (Shpitser & Pearl, 2012). Construction details appear in Appendix D.5; additional background is in Appendix D.

Learning game mechanics. Empirical results highlight the challenges of learning game mechanics. A study performed by Gingerson et al. (2024) highlights the continuing challenge of generating *consistent* gameplay with SOTA architectures—even when generations look plausible, they frequently break the rules of the mechanic. Chen et al. (2025) report similar failures in spatial and numerical consistency, necessitating explicit corrective modules. More broadly, empirical studies of video prediction models show that while they excel in-distribution, they often rely on case-based mimicry and fail under distribution shift, violating simple physical principles (Kang et al., 2024; Riochet et al., 2021).

If we view a mechanic as a latent generative factor, then unsupervised learning of mechanics is provably impossible from video observations of gameplay alone (Locatello et al., 2019) without strong inductive biases (Mitchell, 1980; Wolpert, 1996). Prior work in this area shows that causal representations are at best only partially identifiable from observational data without intervention data or strong causal inductive biases (Spirtes et al., 2000; Bareinboim & Pearl, 2022; Schölkopf et al., 2021). Our work builds on prior work that employs these causal approaches to learning latent generative factors. But to our knowledge, our work is the first to apply this type of causal analysis to the problem of learning game mechanics during training, and generating consistent gameplay from a trained model.

Datasets, testbeds and environments. Existing testbeds, datasets, and environments for world models and video prediction largely emphasize intuitive reasoning about real-world Newtonian physics rather than explicitly defined game mechanics. For instance, IntPhys (Riochet et al., 2018) probes intuitive physics by testing whether models respect basic object permanence and motion, while Physion (Bear et al., 2021) provides simulated videos of collisions and stability events to evaluate physical prediction. However, game mechanics can encompass non-realistic “physics,” such as spell casting and passing through portals. *Multiverse Mechanica* focuses on a broader set of game

Descriptions in Causal Logic	Formal Counterfactual Notation	Consistent Contrast Sample Data
S_1 All else equal, if the opponent has a light weapon, they may equip a shield; if heavy, they cannot.	$\mathcal{S}_1 : P(S_{W=1} = 1, S_{W=0} = 0) \geq \epsilon_1$	$\mathcal{D}_1 = \{\omega_1, C, (S_{W=1}, B_{W=1}, D_{W=1}, V_{W=1}), (S_{W=0}, B_{W=0}, D_{W=0}, V_{W=0})\}$
S_2 All else equal, if the opponent has a shield, they may block; if no shield, they cannot.	$\mathcal{S}_2 : P(B_{S=1} = 1, B_{S=0} = 0) \geq \epsilon_2$	$\mathcal{D}_2 = \{\omega_2, C, W, (B_{S=1}, D_{S=1}, V_{S=1}), (B_{S=0}, D_{S=0}, V_{S=0})\}$
S_3 Given a shield, if a block succeeds then no damage; if it fails, damage occurs.	$\mathcal{S}_3 : P(D_{B=1} = 0, D_{B=0} = 1 S = 1) \geq \epsilon_3$	$\mathcal{D}_3 = \{\omega_3, C, W, S, (D_{B=1}, V_{B=1}), (D_{B=0}, V_{B=0})\}$

Table 2: The shield mechanic described as in natural language causal logic (column 1), which are then formalized with counterfactual notation (column 2), where strictly positive probabilities ($\epsilon_i > 0$) indicate bounded uncertainty due to other causal factors in the system. Column 3 shows *consistent-contrast* tuples (each row shares seed ω_i).

Variable / Operator	Description
$P(X)$	The probability distribution for random variable X
$P(X Z=z)$	As above, but conditioned on observation $Z=z$
$\text{do}(X=x)$	An intervention taken to fix variable X to value x. Interrupts sampling from its conditional probability distribution given parents in the causal DAG: $P(X Pa(X))$.
$P(Y_{X=x} Z=z)$	Probability distribution for Y where an intervention is taken to fix variable X to value x (i.e., $\text{do}(X=x)$) (optionally conditioned on observation $Z=z$)
$\mathcal{S}_i, \mathcal{S}_i$	The i^{th} contrast statement, in causal terms and counterfactual notation, respectively
\mathcal{D}_i	The i^{th} <i>consistent-contrast</i> tuple, defining two worlds sharing a common seed ω_i
X_t, C_t, V_t	Game data at frame t : game state X_t , player controller input C_t , and video frame (image) vector.

Table 3: Key variables and operators used in the adopted formalism.

mechanics, and contributes a *playable generator* that emits data and artifacts that target learning of a formally defined ground-truth set of mechanics.

3 FORMALIZING AND LEARNING A GAME MECHANIC

In this section, we demonstrate the formalization of a game mechanic as well as how we would learn that mechanic from data. Then, in Section 3.2, we provide a general mathematical description of this approach.

3.1 ILLUSTRATING EXAMPLE

The Shield Mechanic Consider a scene from a stylized 90’s fantasy turn-based combat game, where an archer battles a warrior. Like many games in this genre, there is a *shield mechanic*, as shown in Figure 1, where the warrior may raise a shield to block incoming attacks.

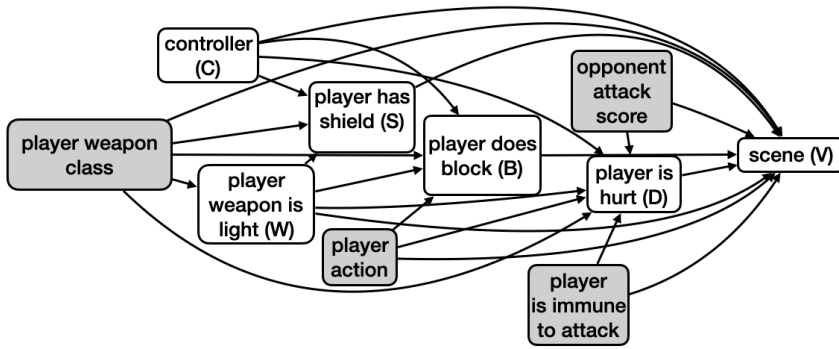
3.1.1 FORMALIZING THE SHIELD MECHANIC

How might we describe this shield mechanic in formal causal terms?

Step 0: Define Notation. As a preliminary step, we define the necessary variables and operators used in our formalism in a notation table (see Table 3).

Step 1: Describe the Mechanic with Causal Logic. We start by completely describing the shield mechanic using a series of causal hypothetical statements of the form “Given preconditions W , all else equal, if X , then Y .” Specifically, we focus on level-3 multiverse logic statements that employ

216
217
218
219
220
221
222
223
224
225
226
227



228 Figure 2: Causal DAG marginalized to focus on the nodes specific to the shield mechanic and their
229 latent confounders (gray nodes)

230
231
232
233
234 conjunctions of conflicting conditions. Table 2 column 1 shows three statements, S_1 , S_2 , and S_3 ,
235 that fully describe the shield mechanic.

236 The columns of Figure 1 correspond to S_1 , S_2 , and S_3 . We could instead use *level-2* interventional
237 statements, which are normally preferred because they are generally testable with experimental data.
238 But the *level-3 parallel world* statements provide an additional constraint in the phrase “all else
239 equal”; that outcomes unaffected by the conditions must remain *consistent* across the clauses. As
240 we will see below, we can use that constraint to operationalize consistency in game generation.
241 Secondly, we can leverage the gaming setting’s rare opportunity to generate level-3 data to validate
242 level-3 statements.

243 **Step 2: Rewrite as Counterfactual Expressions.** We can rewrite S_1 , S_2 , and S_3 as mathemati-
244 cal expressions using counterfactual notation, capturing the contrasts more compactly. For sim-
245 plicity, let W denote the weapon type, S indicate whether a shield is equipped, B indicate whether the
246 shield is used to block, and D indicate whether damage occurs. We treat these as binary variables
247 for clarity, without loss of generality. Let $W = 1$ and $W = 0$ denote light and heavy weapon,
248 respectively. S , B , and D , let 1 mean *True* and 0 mean *False*.

249 We use counterfactual notation to denote variables under the influence of intervention, such that
250 Y under an intervention that sets X to x is written as $Y_{X=x}$. We can formalize the parallel world
251 statements S_1 , S_2 , and S_3 as shown in column 2 of Table 2, where $\epsilon_i; \forall i \in \{1, 2, 3\}$ denotes strictly
252 positive probabilities ($\epsilon_i > 0$), indicating bounded uncertainty due to other causal factors in the
253 system.

254 With this, our shield mechanic is described in formal mathematical terms.

255 **Step 3: Represent Mechanic with Causal Graphs** Let V denote a full clip of gameplay. An
256 outcome, denoted v , is a sequence of frames. Let C denote the controller input from a player at the
257 start of the player’s turn. Let G denote the full causal DAG for a single turn in the battle (see the
258 full graph in Figure 6 in Appendix E). Let us assume we have access to this DAG, or that we could
259 create it using knowledge of the game structure, analyzing causal dependence in the game’s code
260 (Winskel, 1986; Aho et al., 2006), or by applying causal discovery methods (Glymour et al., 2019).
261 The variables implicated in our description of the shield mechanic are $Z = \{C, W, S, B, D, V\}$.
262 The causal DAG G is quite large, so we derive the mDAG G^M that zooms in on Z (Figure 2)
263 by marginalizing out the variables not in Z (see Appendix D.3 for a description of the algorithm).
264 Next, we can combine the mDAG with each counterfactual expression in the mechanic’s description
265 to construct the counterfactual graphs in Figure 3.

266 The counterfactual graphs in Figure 3 encode a representation of *causal consistency*—variables that
267 are not downstream of interventions and thus are consistent across worlds are unique, while incon-
268 sistent variables have nodes indexed by each world. Thus, the counterfactual graphs are representa-
269 tions of the shield mechanic that explicitly describe what should remain consistent when generating
gameplay depicting the shield mechanic.

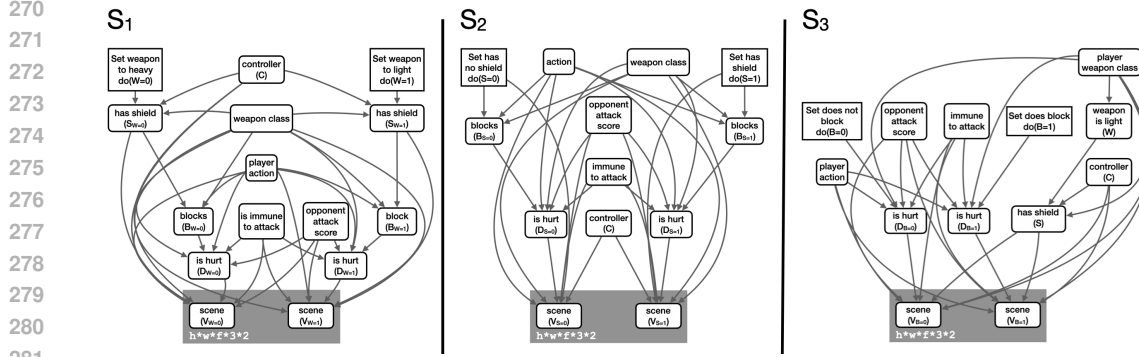


Figure 3: Counterfactual graphs for the shield mechanic. The video variables $V_{X=x}$ have shape height(h)*width(w)*frames(f)*channels(3)*worlds(2).

3.1.2 GENERATING SHIELD MECHANIC DATA

We can generate level-3 parallel world data consistent with S_1 , S_2 , and S_3 by creating parallel runs with identical initial conditions and random seeds. We can intervene separately in each run, producing clips of parallel *virtual* worlds that differ only in their respective interventions. We call the tuple of these clips, combined with the outcomes of other mechanic-related variables under these interventions and their shared initial condition/seed, *consistent contrasts*. Figure 1 illustrates gameplay clips from the contrasts.

Let ω_1 , ω_2 , and ω_3 represent distinct sets of random seeds and initial conditions. Let C represent the controller input from the player. Let $V_{X=x}$ represent a video clip of gameplay under an intervention that sets X to x . Reading consistency from the graphs in Figure 3, we see $W_{S=1} = W_{S=0} = W$, $W_{B=1} = W_{B=0} = W$, and $S_{B=1} = S_{B=0} = S$. Let \mathcal{D}_1 , \mathcal{D}_2 , and \mathcal{D}_3 represent samples of consistent contrasts for S_1 , S_2 , and S_3 respectively, as shown in Table 2 column 3.

3.1.3 LEARNING THE SHIELD MECHANIC FROM DATA

Let $P_1 = P(S_{W=1}, S_{W=0})$, $P_2 = P(B_{S=1}, B_{S=0})$, and $P_3 = P(D_{B=1}, D_{B=0}, S)$ denote the distributions constrained by S_1 , S_2 , and S_3 . We can estimate these distributions through repeated sampling of consistent contrasts \mathcal{D}_1 , \mathcal{D}_2 , and \mathcal{D}_3 , then averaging over the sampling distributions to obtain the sampling distributions \hat{P}_1 , \hat{P}_2 , and \hat{P}_3 (see Appendix D.6). In each case \hat{P}_i converges almost surely to P_i . This provides a precise operationalization of what it means for a generative model to learn the shield mechanic: learning constraints $\{S_1, S_2, S_3\}$ on distributions $\{P_1, P_2, P_3\}$ or modeling $\{P_1, P_2, P_3\}$ directly.

However, in the canonical case of training game world models, we assume that only the controller inputs and the video outputs are observed during training. Here, the inference of \hat{P}_i becomes a task of unsupervised learning of a latent vector $\mathcal{D} \setminus \{C, V_{X=x}, V_{X=x'}\}$ using $\{C, V_{X=x}, V_{X=x'}\}$ as features, where $V_{X=x}, V_{X=x'}$ is a vector of shape $2 * \text{frame height} * \text{frame width} * 3 \text{ RGB channels} * \text{number of frames}$. Without further assumptions, disentangling the components of $\mathcal{D} \setminus \{C, V_{X=x}, V_{X=x'}\}$ is generally infeasible. However, the counterfactual graphs in Figure 3 already disentangle these variables for us. Using these, the problem reduces to training a latent variable model.

3.2 FORMAL FRAMEWORK FOR GAME MECHANICS

We assume a causal DAG $G = (V, E)$ for a single step of gameplay with $V = \{C_t, X_t, C_{t+1}, X_{t+1}, V_t, V_{t+1}\}$, and typical edges $X_t \rightarrow C_t$, $X_t \rightarrow X_{t+1}$, $C_t \rightarrow X_{t+1}$, $X_t \rightarrow V_t$, $X_{t+1} \rightarrow V_{t+1}$. For a given mechanic, we restrict to the variable subset $M = \{C_t, X_t^M, X_{t+1}^M, V_{t+1}\}$, $X_t^M \subseteq X_t$, $X_{t+1}^M \subseteq X_{t+1}$, and form the marginalized DAG G^M by marginalizing variables outside M while preserving interventional semantics (Appendix D.3).

We work on a probability space with sample space Ω . Each variable $Z \in M$ is a measurable mapping $Z : \Omega \rightarrow \mathcal{X}_Z$, and each counterfactual $Z_{X=x} : \Omega \rightarrow \mathcal{X}_Z$, where $x \in \mathcal{X}_X$ is an intervention

324 value in the state space of X . The ground-truth SCM, consistent with G^M , induces the family
 325

$$326 \quad \mathcal{F}(M) = \left\{ P(V_{t+1, X=x}, Z_{X=x} \mid E) : X, Z \in M, x \in \mathcal{X}_X, E \in \sigma(M) \right\}, \\ 327$$

328 where $\sigma(M)$ denotes the σ -algebra generated by the variables in M (in practice, E can be any
 329 measurable predicate on M , e.g., $S=1$ for “has shield”).
 330

331 We formalize a mechanic as the tuple $\langle G^M, \mathcal{M} \rangle$, where $\mathcal{M} = \{S_1, \dots, S_k\}$ and each constraint
 332 $\mathcal{S}_i : P\left(\bigwedge_{j=1}^{m_i} Y_{X=x_j} = y_j \mid E\right) \geq \epsilon_i$ binds counterfactuals of variables in M under inter-
 333 ventions on $X \in M$, with $x_j \in \mathcal{X}_X$, $E \in \sigma(M)$, and $\epsilon_i \in (0, 1]$ (allowing non-deterministic
 334 relations due to factors outside M). For each \mathcal{S}_i we denote the targeted distribution by P_i (e.g.,
 335 $P_1 = P(S_{W=1}, S_{W=0})$ in the shield example).
 336

337 **Data and Estimation.** A consistent-contrast dataset for \mathcal{S}_i of size N is
 338

$$339 \quad \mathcal{D}_i^{(N)} = \left\{ (V_{X=x_1}(\omega_n), \dots, V_{X=x_{m_i}}(\omega_n)) : \omega_n \in \Omega, n = 1, \dots, N \right\}, \\ 340$$

341 optionally restricted to ω_n satisfying E . Let $\hat{P}_i^{(N)}$ be the empirical distribution induced by $\mathcal{D}_i^{(N)}$.
 342 Under i.i.d. sampling of seeds ω_n , $\hat{P}_i^{(N)} \xrightarrow{\text{a.s.}} P_i$. For each \mathcal{S}_i (and associated P_i), we construct a
 343 *counterfactual graph* $G_i^{M, \text{cf}}$. In partially observed settings (video + controller only), G_i^{cf} specifies
 344 which latent variables are shared across worlds and which differ, reducing estimation to a well-posed
 345 latent variable problem aligned with the counterfactual graph’s structure.
 346

347 4 MULTIVERSE MECHANICA: A PLAYABLE TESTBED FOR LEARNING 348 MECHANICS

351 We introduce *Multiverse Mechanica*, a fantasy-style battle game designed as a testbed for learning
 352 game mechanics. Unlike static datasets, Multiverse Mechanica is a playable game that emits the
 353 artifacts required to study and evaluate whether models capture the game’s mechanics—not just
 354 gameplay visuals. Its design integrates three innovations: (i) native support for level-3 parallel-
 355 world contrasts with consistency under the same ω ; (ii) per-mechanic mDAGs G^M , parallel world
 356 and counterfactual graphs, and specifications of \mathcal{M} ; and (iii) explicit visual grounding, where stance
 357 and scene variables are rendered into pixels. We will release the game upon publication.
 358

359 4.1 GAME OVERVIEW

361 Each episode consists of a pre-battle setup (character and equipment selection, random assignment
 362 of elemental buffs (e.g., fire, ice) followed by turn-based combat. The player occupies the left side
 363 of the screen, and the enemy occupies the right. On the player’s turn to attack, a timing-based
 364 interaction yields an attack score; the enemy’s turn samples an analogous attack score. Outcomes
 365 depend on weapons, defenses, the attack score, and buffs. See Appendix F for additional details.
 366

367 4.2 IMPLEMENTED MECHANICS (v1.0)

369 Version 1.0 of Multiverse Mechanica includes the following mechanics, each with associated
 370 G^M and parallel-world data sufficient to estimate \mathcal{M} . The **shield mechanic** focuses on equipping
 371 and blocking with a shield, as discussed in Section 3.1. In the **elemental immunity mechanic**, “elemental” attributes (e.g., fire and ice) govern immunity and vulnerability to attacks. The
 372 **weapon range mechanic** governs melee vs. ranged combat. The **spell-casting mechanic** governs
 373 five submechanics that allow players to give themselves an advantage in battle (e.g., gain
 374 increased attack power, dodge ability), or their opponent a disadvantage (e.g., disarm them or
 375 lower their defense)—projectiles, self-levitation, enemy-levitation, self-transformation, and enemy-
 376 transformation. See Appendix E for detailed descriptions, including causal formalizations, DAGs,
 377 and illustrations.

378
379

4.3 DESIGN DECISIONS

380
381
382

Mechanic-Specific Game Systems. Each mechanic is implemented with a unique instance of a *game system* (Nystrom, 2014; Gregory, 2018), independent of the others. This ensures parity between the mechanic and the code logic. Full game system details are given in Appendix F.1.1.

383
384
385
386
387

Impact Frames and Visual Conventions. We designed the game such that each turn contains an *impact frame*—the most visually and mechanically expressive phase of an interaction (e.g., the precise moment when an attack lands) Impact frames are not based on fixed time-points but are set according to specific conditions in the finite-state machines. See Appendix F.2 for details.

388
389
390
391
392
393
394
395
396

Simple yet Information Dense Visuals. To facilitate rapid, inexpensive experimentation, we focus on the ability to run experiments with episodes that have a minimal number of frames. To this end, we use a simple art style that aligns with the representational biases of pretrained vision models (lucII, 2024; Zhang et al., 2023) and animation conventions that emphasize dynamic information, such as speed lines (“zip ribbons”) to depict fast motion, trajectory lines for projectiles, curved swipes for melee attacks, and burst lines and explosion visual effects for collisions or blocked strikes (McCloud, 2020; Eisner, 2008; Cohn, 2013). In Section 5, we highlight this ability by limiting our analysis to single time-point snapshots at the impact frame, chosen as the impact frame of the clip. The images in Figure 1 are all sampled at their respective impact frames.

397
398

4.4 DATA GENERATION

399
400
401
402
403
404
405
406
407
408
409

Multiverse Mechanica is not a dataset but a generator. To generate data, an automated agent repeatedly plays the game to produce clips. Users can select a number N of generations. The generation process can randomly generate N clip examples, constituting level-1 data. The user can also specify interventions on specific game state variables and generate N clip examples where those interventions are applied, constituting level-2 data. Finally, the user can specify interventions and assign them to multiple game instances with a shared “ ω ” (same random seed and initial conditions) and generate N consistent contrasts (tuples of clips), constituting level-3 data. Each mechanic has presets for level-2 and level-3 generation. Each clip is a 512x512 MP4 video averaging 4 seconds at 50 FPS. Each generated example is a tuple consisting of a clip, controller inputs, game-state variable outcomes, and a random seed for reproducibility. See Appendix G for additional details related to data generation.

410
411
412
413

Summary. Multiverse Mechanica provides a compact yet expressive testbed for studying whether generative models can capture mechanics. Its design couples causal structure with visual grounding, leverages art and animation conventions for low-cost training, and enables reproducible creation of parallel-world contrasts.

414
415
416
4175 PROOF-OF-CONCEPT: LEARNING A MECHANIC WITH DIFFUSION
FINE-TUNING418
419
420
421
422
423
424

One advantage of *Multiverse Mechanica*’s design (Section 4.3) is that mechanics are rendered into *impact frames* using simple yet information-dense visuals. This allows experiments with supervision from clips as short as a single frame. We illustrate this with a case study: fine-tuning a pretrained image diffusion model to target mechanic learning. Specifically, we fine-tune the model to learn the full mechanic set (i.e., shield, elemental immunity, weapon range, and spell-related submechanics), as discussed in Section 4.2.

425
426
427
428
429

We fine-tuned the latent diffusion model *OpenJourney-v4* (PromptHero, 2022) on $N = 1000$ impact frame *consistent contrasts* generated from the game. Each consistent contrast consists of paired images $(V_{X=x_0}, V_{X=x_1})$ from parallel worlds that share a random seed ω but differ by interventions on a mechanic variable X . This setup directly instantiates the causal consistency principle: non-descendant variables of X should remain invariant across the pair.

430
431

We introduce a **multiverse alignment** objective—a modification of the standard diffusion loss—to enforce the *causal consistency principle*. In a consistent contrast, all elements share a common sample $\omega \in \Omega$, mirroring the reverse process in deterministic diffusion variants that generate data



Figure 4: Proof-of-concept of shield mechanic learning with a diffusion model trained on game data. Mechanic learning is shown by sampling counterfactuals: unchanged image elements remain consistent with the original. (A) Held-out game image: wizard attacks warrior (blue due to an ice elemental buff). (B) Generated counterfactual with warrior holding a shield but not blocking ($V_{S=1, B=0}$). (C) Generated counterfactual with shield and block active ($V_{S=1, B=1}$) (aliased sword is a generation error).

from latent noise. We therefore initialize each contrast trajectory with the *same* noise: sample $\omega \sim \mathcal{N}(0, I)$ and set $Z_{T, X=x_0} = Z_{T, X=x_1} = \omega$.

Let $\{X = x_0, V_{X=x_0}, X = x_1, V_{X=x_1}\} \sim \hat{P}$, where $X \in \mathcal{X}_X$ is a game-state variable under intervention and $V_{X=x_j}$ is the corresponding impact frame snapshot under intervention $X = x_j$. With timesteps $t \in [0, T]$, let $Z_{t, X=x_0}, Z_{t, X=x_1}$ denote the noisy latent representations of $V_{X=x_0}$ and $V_{X=x_1}$, respectively. Conditioned on controller input c , the *denoiser* $\epsilon_\theta(\cdot)$ iteratively transforms the shared seed ω into a clean latent $Z_{0, X=x_j}$ that decodes into the impact frame $V_{X=x_j}$. Our task is to train the denoiser’s weights θ with a loss that enforces causal consistency across contrasts.

The **multiverse alignment** loss has two components:

$$\mathcal{L} = \lambda_1 \mathcal{L}_1 + \lambda_2 \mathcal{L}_2, \quad \lambda_1, \lambda_2 \geq 0, \quad \lambda_1 + \lambda_2 = 1.$$

\mathcal{L}_1 : seed-consistency loss. Let Abduct_θ denote an inversion procedure that estimates the Gaussian seed from an observed impact-frame latent $Z_{0, X=x_j}$ and controller input c_j . Given $Z_{0, X=x_j}$ with controller input c_j , Abduct_θ uses the denoiser $\epsilon_\theta(\cdot)$ to trace $Z_{t, X=x_j}$ backward through the noise schedule, producing an estimate $\hat{\omega}_j$ of the exogenous seed ω . Under a deterministic sampler (e.g., DDIM), this corresponds to following the reverse trajectory from the observed latent to the initial noise (see Appendix I.10.5 for details). The seed-consistency loss then enforces agreement between abducted seeds across a consistent contrast:

$$\mathcal{L}_1(Z_{0, X=x_0}, c_0, Z_{0, X=x_1}, c_1) = \|\text{Abduct}_\theta(Z_{0, X=x_0}, c_0) - \text{Abduct}_\theta(Z_{0, X=x_1}, c_1)\|_2^2.$$

Remark. With deterministic sampling, shared ω implies shared non-descendant content. Minimizing \mathcal{L}_1 suppresses nuisance differences and attributes variation to mechanic-specific interventions.

\mathcal{L}_2 : structure-alignment loss. Let $S \subset \{1, \dots, T\}$ be a subset of high-noise timesteps. For each $t \in S$, the denoiser predicts noise $\epsilon_\theta(Z_{t, X=x_j}, t, c_j)$. We align predictions across the contrast:

$$\mathcal{L}_2 = \sum_{t \in S} \|\epsilon_\theta(Z_{t, X=x_0}, t, c_0) - \epsilon_\theta(Z_{t, X=x_1}, t, c_1)\|_2^2.$$

Remark. Early reverse steps encode coarse layout. Aligning them enforces global semantic identity across contrasts, while leaving mechanic-specific differences to emerge in later, low-noise steps.

Evaluation Results.

Figure 4 shows qualitative counterfactual generations: the model preserves non-mechanic-related content while toggling the targeted shield mechanic. From a factual image v with $X = x$ we abduct the exogenous seed ω , then generate a counterfactual image v' with $X = x'$ while keeping ω fixed. This corresponds to sampling from $P(V_{X=x'} | X = x, V = v)$, i.e. counterfactual reconstruction with shared ω . This provides visual evidence that the fine-tuned model has learned aspects of the mechanic, not merely pixels.

To systematize this evaluation, we report quantitative results in Table 4. The causal consistency metrics provide a systematic approach to evaluating consistency (Hessel et al., 2021; Radford et al.,

486 2021), and we include metrics for image quality and reconstruction quality (Wang et al., 2004;
 487 Wolf et al., 2009) to serve as table-stakes baselines. While the model demonstrates reasonable
 488 image-to-text alignment (CLIP score: 24.45) and strong image similarity (0.89) between factual and
 489 counterfactual pairs, the reconstruction metrics reveal challenges in perfectly inverting the diffusion
 490 process, with reconstruction PSNR at 10.73 dB. The high exogenous distance (0.67) suggests that
 491 our current implementation requires further optimization to achieve tighter alignment between par-
 492 allel worlds. Despite these limitations, the model successfully generates semantically meaningful
 493 counterfactuals, as evidenced by the transfer CLIP score of 20.77.

494

495 Table 4: Evaluation metrics for diffusion fine-tuning on 1000 consistent-contrast pairs. Causal
 496 consistency is emphasized as the key criterion for mechanic learning; reconstruction and image
 497 quality provide baseline checks.

498

Metric Category	Metric	Value
Causal Consistency	CF Transfer CLIP Score	20.77
	Exogenous Distance (MSE)↓	0.671
Reconstruction	Reconstruction PSNR	10.73 dB
	Reconstruction SSIM	0.183
	Reconstruction CLIP Score	21.45
Image Quality	PSNR (Factual vs CF)	17.66 dB
	SSIM (Factual vs CF)	0.433
	CLIP Image-Text Score	24.45
	CLIP Image-Image Similarity	0.892

500

501

502

503

504

505

506

507

508

509

6 SCALABILITY & LIMITATIONS

513

514

515 Our descriptions of mechanics assume parallel-world statements (Section 3.1) with discrete differ-
 516 ences across worlds; the same logic extends to incremental changes, but we have not yet charac-
 517 terized which mechanics require that expressivity. In our proof-of-concept, we operate on impact
 518 frame snapshots (Section 5), which makes experiments tractable but sidesteps temporal dynamics.
 519 Although our current evaluation is limited to settings with similar temporal structure, in principle,
 520 the approach applies to any generative video model capable of conditioning across worlds. As future
 521 work, we plan to benchmark video-capable world models and longer horizons.

522

523

524 Contrast generation scales linearly with the number of worlds per mechanic and seeds, whereas
 525 composing multiple mechanics can grow contrasts combinatorially. Our simplified 2D domain re-
 526 duces compute expense and aids clarity, but limits transfer to photorealistic 3D and other genres,
 527 where new rendering conditions and longer horizons demand more complex models. Evaluation of
 528 consistency currently relies on human or VLM-based checks; the robustness of automated evaluators
 529 in this setting remains an open challenge.

530

531

532

533

534

535

536

537

538

539

530 Beyond video games, our causal-consistency formulation—which expresses mechanics as coun-
 531 terfactual constraints over an SCM and enforces cross-world consistency—extends to other con-
 532 trollable simulators and content-generation pipelines. Many physics engines, animation systems,
 533 and VFX toolchains expose structured state, deterministic updates, and seed-controlled stochas-
 534 ticity, providing the ingredients needed to construct parallel-world contrasts. In these settings,
 535 “mechanics” may correspond to physical laws, interaction rules, or rendering effects. However,
 536 realistic simulators involve high-dimensional latent state, longer temporal dependencies, and ren-
 537 dering stacks whose stochasticity may not align cleanly across worlds; likewise, real-world video
 538 lacks explicit multiverse structure, often requiring synthetic contrasts or approximate consistency
 539 objectives. Thus, while *Multiverse Mechanica* provides a “best-case” environment where contrasts
 are explicit, extending these ideas to more complex simulators or cinematic pipelines will require
 domain-specific approximations and strategies for generating or inferring multiverse-like structure.

540 7 CONCLUSION
541

542 We formalized game mechanics as causal counterfactual inference and introduced *Multiverse Me-*
543 *chanica*, a playable testbed that emits parallel-world contrasts and per-mechanic causal graphs.
544 Building on this foundation, we proposed a multiverse-alignment objective and demonstrated a
545 proof-of-concept fine-tuning that learns targeted mechanics. Together, these components provide
546 a reproducible path to assessing whether world models learn *mechanics—not just pixels*.

548 REFERENCES
549

550 Alfred V. Aho, Monica S. Lam, Ravi Sethi, and Jeffrey D. Ullman. *Compilers: Principles, Tech-*
551 *niques, and Tools*. Addison-Wesley, Boston, MA, 2nd edition, 2006. ISBN 9780321486813.

552 E. Bareinboim and J. Pearl. *Causal Inference and the Data-Fusion Problem*. Cambridge University
553 Press, 2022. ISBN 9781108844984.

555 Elias Bareinboim, Juan D. Correa, Duligur Ibeling, and Thomas Icard. On pearl’s hierarchy and
556 the foundations of causal inference. In Hector Geffner, Rina Dechter, and Joseph Y. Halpern
557 (eds.), *Probabilistic and Causal Inference: The Works of Judea Pearl*, pp. 507–556. Association
558 for Computing Machinery, New York, NY, USA, 2022. ISBN 9781450395861. doi: 10.1145/
559 3501714.3501737.

560 Daniel M Bear, Elias Wang, Damian Mrowca, Felix J Binder, Hsiao-Yu Fish Tung, RT Pramod,
561 Cameron Holdaway, Sirui Tao, Kevin Smith, Fan-Yun Sun, et al. Physion: Evaluating physical
562 prediction from vision in humans and machines. *arXiv preprint arXiv:2106.08261*, 2021.

563 Eli Bingham, Jonathan P Chen, Martin Jankowiak, Fritz Obermeyer, Neeraj Pradhan, Theofanis
564 Karaletsos, Rohit Singh, Paul Szerlip, Paul Horsfall, and Noah D Goodman. Pyro: Deep universal
565 probabilistic programming. *Journal of machine learning research*, 20(28):1–6, 2019.

567 Staffan Björk and Jussi Holopainen. *Patterns in Game Design*. Charles River Media, Hingham,
568 MA, 2004. ISBN 1-58450-354-8.

569 Stephan Bongers, Tineke Blom, and Joris M Mooij. Causal modeling of dynamical systems. *arXiv*
570 *preprint arXiv:1803.08784*, 2018.

572 Jake Bruce, Michael D Dennis, Ashley Edwards, Jack Parker-Holder, Yuge Shi, Edward Hughes,
573 Matthew Lai, Aditi Mavalankar, Richie Steigerwald, Chris Apps, et al. Genie: Generative inter-
574 active environments. In *Forty-first International Conference on Machine Learning*, 2024.

576 Haoxuan Che, Xuanhua He, Quande Liu, Cheng Jin, and Hao Chen. Gamegen-x: Interactive open-
577 world game video generation. In *International Conference on Learning Representations*, 2025.
578 URL <https://openreview.net/forum?id=8VG8tpPZhe>.

579 Z. Chen, T. Xu, Y. Zhang, et al. Model as a game: On numerical and spatial consistency for gen-
580 erative games. *arXiv preprint arXiv:2503.21172*, 2025. URL <https://arxiv.org/abs/2503.21172>.

582 Neil Cohn. *The Visual Language of Comics: Introduction to the Structure and Cognition of Sequen-*
583 *tial Images*. Bloomsbury Advances in Semiotics. Bloomsbury Academic, London, 2013. ISBN
584 9781472542175.

586 Decart, Julian Quevedo, Quinn McIntyre, Spruce Campbell, Xinlei Chen, and Robert Wachen. Oa-
587 sis: A universe in a transformer. <https://oasis-model.github.io/>, 2024. Accessed:
588 2025-09-24.

589 Joris Dormans. *Engineering Emergence: Applied Theory for Game Design*. PhD thesis, University
590 of Amsterdam, 2012. URL <https://eprints.illc.uva.nl/id/eprint/2118/1/DS-2012-12.text.pdf>.

593 Will Eisner. *Comics & Sequential Art*. W. W. Norton & Company, New York, revised edition edition,
2008. ISBN 9780393331264. First published 1985; expanded edition 1990; revised edition 2008.

594 Robin J Evans. Graphs for margins of bayesian networks. *Scandinavian Journal of Statistics*, 43(3):
 595 625–648, 2016.

596

597 Carlo Fabricatore. Gameplay and game mechanics: A key to quality in videogames. In *Proc. OECD*
 598 *Expert Meeting on Videogames and Education*, 2007. URL <https://eprints.hud.ac.uk/id/eprint/20927/>.

599

600 Tracy Fullerton, Chris Swain, and Steven Hoffman. *Game design workshop: Designing, prototyp-*
 601 *ing, & playtesting games*. CRC Press, 2004.

602

603 J. Gingerson, S. Amershi, et al. World and human action models towards gameplay ideation. *Nature*,
 604 2024. URL <https://www.nature.com/articles/wham2024>. Microsoft Research
 605 technical report also available.

606 Clark Glymour, Kun Zhang, and Peter Spirtes. Review of causal discovery methods based on graph-
 607 ical models. *Frontiers in genetics*, 10:524, 2019.

608

609 Jason Gregory. *Game Engine Architecture*. A K Peters/CRC Press, Boca Raton, FL, 3 edition, 2018.
 610 ISBN 9781138035454.

611

612 David Ha and Jürgen Schmidhuber. World models. *arXiv preprint arXiv:1803.10122*, 2018. URL
 613 <https://arxiv.org/abs/1803.10122>.

614

615 Xianglong He, Chunli Peng, Zexiang Liu, Boyang Wang, Yifan Zhang, Qi Cui, Fei Kang, Biao
 616 Jiang, Mengyin An, Yangyang Ren, Baixin Xu, Hao-Xiang Guo, Kaixiong Gong, Cyrus Wu,
 617 Wei Li, Xuchen Song, Yang Liu, Eric Li, and Yahui Zhou. Matrix-game 2.0: An open-source,
 618 real-time, and streaming interactive world model. *arXiv preprint arXiv:2508.13009*, 2025.

619

620 Mariya Hendriksen, Tabish Rashid, David Bignell, Raluca Georgescu, Abdelhak Lemkhenter, Katja
 621 Hofmann, Sam Devlin, and Sarah Parisot. Adapting vision-language models for evaluating world
 622 models. *arXiv preprint arXiv:2506.17967*, 2025.

623

624 Jack Hessel, Ari Holtzman, Maxwell Forbes, Ronan Le Bras, and Yejin Choi. Clipscore: A
 625 reference-free evaluation metric for image captioning. In *Proceedings of the 2021 Conference*
 626 *on Empirical Methods in Natural Language Processing (EMNLP)*, pp. 7514–7528, 2021. doi:
 627 10.18653/v1/2021.emnlp-main.595.

628

629 Paul W. Holland. Statistics and causal inference. *Journal of the American Statistical Association*,
 630 81(396):945–960, 1986. doi: 10.2307/2289064.

631

632 Charles Tapley Hoyt, Craig Bakker, Richard J. Callahan, Joseph Cottam, August George, Ben-
 633 jamin M. Gyori, Haley M. Hummel, Nathaniel Merrill, Sara Mohammad Taheri, Pruthvi Prakash
 634 Navada, Marc-Antoine Parent, Adam Rupe, Olga Vitek, and Jeremy Zucker. Causal Iden-
 635 tification with Y_0 , 2025. URL <https://doi.org/10.48550/arXiv.2508.03167>.
 636

637

638 Robin Hunicke, Marc LeBlanc, and Robert Zubek. MDA: A formal ap-
 639 proach to game design and game research. In *Proc. AAAI Workshop on*
 640 *Challenges in Game AI*, 2004. URL <https://aaai.org/papers/ws04-04-001-md-a-formal-approach-to-game-design-and-game-research/>.

641

642 Aki Järvinen. *Games without Frontiers: Theories and Methods for Game Studies and Design*. PhD
 643 thesis, University of Tampere, 2008. URL https://ocw.metu.edu.tr/pluginfile.php/4468/mod_resource/content/0/ceit706/week3_new/AkiJarvinen_Dissertation.pdf.

644

645 D. Kang, Y. Wu, et al. How far is video generation from world models? *arXiv preprint*
 646 *arXiv:2402.19014*, 2024. URL <https://arxiv.org/abs/2402.19014>.

647

648 Tero Karras, Miika Aittala, Timo Aila, and Samuli Laine. Elucidating the design space of diffusion-
 649 based generative models. *Advances in neural information processing systems*, 35:26565–26577,
 650 2022.

648 Seung Wook Kim, Yuhao Zhou, Jonah Philion, Antonio Torralba, and Sanja Fidler. Learning to
 649 simulate dynamic environments with gamegan. In *Proc. IEEE/CVF Conference on Computer*
 650 *Vision and Pattern Recognition (CVPR)*, 2020. URL https://openaccess.thecvf.com/content_CVPR_2020/papers/Kim_Learning_to_Simulate_Dynamic_Environments_With_GameGAN_CVPR_2020_paper.pdf.

653 Priscilla Lo, David Thue, and Elin Carstensdottir. What is a game mechanic? In *International*
 654 *Conference on Entertainment Computing*, pp. 336–347. Springer, 2021.

655 F. Locatello, S. Bauer, M. Lucic, G. Raetsch, S. Gelly, B. Schölkopf, and O. Bachem. Chal-
 656 lenging common assumptions in the unsupervised learning of disentangled representations. In
 657 *Proceedings of the 36th International Conference on Machine Learning (ICML)*, 2019. URL
 658 <https://arxiv.org/abs/1811.12359>.

660 luciI. Chibi artstyle model. <https://civitai.com/models/22820/chibi-artstyle>,
 661 2024. Community submission on Civitai. Accessed: 2025-09-24.

662 Sus Lundgren and Staffan Bjork. Game mechanics: Describing computer-augmented games in terms
 663 of interaction. In *Proceedings of TIDSE*, volume 3, 2003.

665 Scott McCloud. *Understanding Comics: The Invisible Art*. Harper Perennial, reprint edition edition,
 666 2020. ISBN 9780060976255.

667 T. M. Mitchell. *The Need for Biases in Learning Generalizations*. Technical Report CBM-TR-117,
 668 Rutgers University, 1980.

670 Miguel Monteiro, Fabio De Sousa Ribeiro, Nick Pawlowski, Daniel C Castro, and Ben
 671 Glocker. Measuring axiomatic soundness of counterfactual image models. *arXiv preprint*
 672 *arXiv:2303.01274*, 2023.

673 Robert Nystrom. *Game Programming Patterns*. Genever Benning, 2014. ISBN 9780990582908.

674 Jack Parker-Holder and Shlomi Fruchter. Genie 3: A new frontier for world models. Google
 675 DeepMind Blog, aug 2025. URL <https://deepmind.google/discover/blog/genie-3-a-new-frontier-for-world-models/>. Accessed 24 September 2025.

676 Judea Pearl. *Causality*. Cambridge university press, 2009.

677 Judea Pearl. On the consistency rule in causal inference: axiom, definition, assumption, or theorem? *Epidemiology*, 21(6):872–875, 2010.

678 PromptHero. Openjourney v4. <https://huggingface.co/prompthero/openjourney-v4>, 2022. Diffusion model hosted on Hugging Face.

679 Alec Radford, Jong Wook Kim, Chris Hallacy, Aditya Ramesh, Gabriel Goh, Sandhini Agar-
 680 wal, Girish Sastry, Amanda Askell, Pamela Mishkin, Jack Clark, Gretchen Krueger, and Ilya
 681 Sutskever. Learning transferable visual models from natural language supervision. In *Proceedings*
 682 *of the 38th International Conference on Machine Learning (ICML)*, volume 139, pp. 8748–8763.
 683 PMLR, 2021. URL <http://proceedings.mlr.press/v139/radford21a.html>.

684 J. Riochet, H. Le Borgne, E. Ricci, et al. Intphys 2: A benchmark for physical consistency in
 685 video prediction. In *Proceedings of the IEEE/CVF International Conference on Computer Vision*
 686 (*ICCV*), 2021. URL <https://arxiv.org/abs/2107.06227>.

687 Ronan Riochet, Mario Ynocente Castro, Mathieu Bernard, Adam Lerer, Rob Fergus, Véronique
 688 Izard, and Emmanuel Dupoux. Intphys: A framework and benchmark for visual intuitive physics
 689 reasoning. *arXiv preprint arXiv:1803.07616*, 2018.

690 Tom Schaul. A video game description language for model-based or interactive learning. In
 691 *Proceedings of the IEEE Conference on Computational Intelligence in Games*, 2013. URL
 692 <https://schaul.site44.com/publications/pyvgdl.pdf>.

693 B. Schölkopf, F. Locatello, S. Bauer, N. R. Ke, N. Kalchbrenner, A. Goyal, and Y. Bengio. Towards
 694 causal representation learning. *Proceedings of the IEEE*, 109(5):612–634, 2021. doi: 10.1109/JPROC.2021.3058954.

702 Ilya Shpitser and Judea Pearl. What counterfactuals can be tested. *arXiv preprint arXiv:1206.5294*,
 703 2012.

704

705 P. Spirtes, C. Glymour, and R. Scheines. *Causation, Prediction, and Search*. MIT Press, 2nd edition,
 706 2000. ISBN 9780262194402.

707 Michael Thielscher. The general game playing description language is universal. In *Proceedings of*
 708 *the 22nd International Joint Conference on Artificial Intelligence (IJCAI)*, 2011. URL <https://www.ijcai.org/Proceedings/11/Papers/189.pdf>.

709

710 Zhou Wang, Alan C. Bovik, Hamid R. Sheikh, and Eero P. Simoncelli. Image quality assessment:
 711 From error visibility to structural similarity. *IEEE Transactions on Image Processing*, 13(4):
 712 600–612, 2004. doi: 10.1109/TIP.2003.819861.

713

714 Glynn Winskel. Event structures. In *Advanced course on Petri nets*, pp. 325–392. Springer, 1986.

715

716 Stephen Wolf, Margaret Pinson, et al. Reference algorithm for computing peak signal to noise ratio
 717 (psnr) of a video sequence with a constant delay. Technical Report NTIA/ITS / COM-9 C.6,
 718 National Telecommunications and Information Administration (NTIA) / ITS, 2009. Proposed
 719 reference implementation and calibration procedures for PSNR.

720

721 D. H. Wolpert. The lack of a priori distinctions between learning algorithms. *Neural Computation*,
 722 8(7):1341–1390, 1996. doi: 10.1162/neco.1996.8.7.1341.

723

724 Lvmin Zhang, Anyi Rao, and Maneesh Agrawala. Adding conditional control to text-to-image
 725 diffusion models. In *Proceedings of the IEEE/CVF International Conference on Computer Vision*
 726 (ICCV), pp. 3813–3824. IEEE, 2023. ISBN 9798350307184. doi: 10.1109/ICCV51070.2023.
 00355.

727

728 Alexander Zook and Mark Riedl. Automatic game design via mechanic generation. In *Proceedings*
 729 *of the AAAI Conference on Artificial Intelligence*, volume 28, 2014.

730

731 Alexander Zook and Mark O. Riedl. Automatic game design via mechanic generation. *arXiv*
 732 preprint *arXiv:1908.01420*, 2019. URL <https://arxiv.org/abs/1908.01420>.

733

A USE OF LARGE LANGUAGE MODELS (LLMs)

734

735 GPT-5 was used for editing and polishing during the writing of this paper. The LLM was not used
 736 to make any technical or scientific contributions to the paper writing process; for example: writing
 737 the literature review or background sections, creating citations, or analyzing data.

738

B ETHICS STATEMENT

739

740 There are no ethics concerns raised by this paper.

741

C REPRODUCIBILITY STATEMENT

742

743 To ensure reproducibility of this paper, we make the following efforts:

744

- 745 • We will release Multiverse Mechanica upon publication to provide researchers a game for
 746 use as a testbed for evaluating learning of game mechanics.
- 747 • We will make available publicly upon publication the dataset (including mechanism-
 748 specific graphical artifacts) used for the proof-of-concept training presented in Section 5.

749

C.1 PROOF-OF-CONCEPT DATASET

750

751 Here, we describe the dataset used for the proof-of-concept training presented in Section 5, used to
 752 learn the **shield gameplay mechanic**.

753

756
757
758
759
760
761
762
763
764
765
766
767
768
769
770
771
772
773
774
775
776



777 Figure 5: Impact frame generated by Multiverse Mechanica for a world in a parallel world tuple.
778
779

780 C.1.1 GENERATION

781 We generate a level-3 dataset, as described in Section 4.4. We automatically derive parallel world
782 interventions based on the full game DAG, targeting the variables relevant to the parallel world
783 contrast statements for the shield mechanic. The set of derived interventions define multiple parallel
784 world tuples, enumerated such that we sufficiently cover the support of joint distribution of the
785 mDAG induced by the query variables associated with the level-3 parallel world statements for the
786 mechanic.

787 We assign these interventions to multiple game instances with a shared “ ω ” (same random seed and
788 initial conditions) and generate $N = 1000$ consistent contrasts, constituting level-3 data. Since we
789 are training on text and images (i.e., not gameplay clips), for each we generate only a subset of
790 training artifacts consisting of these two modalities: 1) the impact frame as a 512x512 PNG image,
791 and 2) the game-state variable outcomes (converted into a caption in the pre-processing method,
792 outlined below).

793 C.1.2 PRE-PROCESSING

794 To align our artifact modalities with the text-to-image latent diffusion architecture used in our proof-
795 of-concept, we must perform a pre-processing step to convert from the game-state variable out-
796 comes—a dictionary of variable-name/value pairs—to a text caption. We implement a templated
797 captioning process for each parallel world tuple, by which plain-text captions are deterministically
798 constructed based on the values of the game-state variables.

801 Consider, for example, the following impact frame image and game-state variable artifacts generated
802 by Multiverse Mechanica for one of the worlds in a parallel world tuple.

803 For this world, Multiverse Mechanica has generated the impact frame image shown in Figure 5 and
804 the following game-play state:

```
805
806 gameplay_state = {
807     'background': 'forest',
808     'player action': 'melee attack',
809     'player class': 'warrior',
810     'player does block': False,
811     'player element': 'ice',
```

```

810     'player has shield': False,
811     'player is hurt': False,
812     'player is immune to attack': False,
813     'player weapon': 'short sword',
814     'player weapon class': 'light',
815     'player weapon element': 'ice',
816     'player weapon is light': True,
817     'player weapon range': 'melee',
818     'opponent action': 'defend',
819     'opponent class': 'warrior',
820     'opponent does block': True,
821     'opponent element': 'none',
822     'opponent has shield': True,
823     'opponent is hurt': False,
824     'opponent is immune to attack': False,
825     'opponent weapon': 'short sword',
826     'opponent weapon class': 'light',
827     'opponent weapon element': 'fire',
828     'opponent weapon is light': True,
829     'opponent weapon range': 'melee',
830 }
```

Given this game-play state, our pre-processing step constructs the following caption:

831 “A 1-on-1 battle between two warriors. The warrior on the left has a ice element
832 buff. The warrior on the left’s weapon is a short sword with a ice buff. The warrior
833 on the left is launching a melee attack. The warrior on the right’s weapon is a short
834 sword with a fire buff and they have a shield. The warrior on the right is blocking
835 with their shield.”

The captions generated by the pre-processing step is combined with the generated image to thus create training data suitable for text-to-image latent diffusion architecture used in our proof-of-concept.

D BRIEF PRIMER ON CORE CAUSAL CONCEPTS

D.1 THE CAUSAL HIERARCHY

The *causal hierarchy* describes three levels of statements that employ causal logic: (level-1) observation, (level-2) intervention, and (level-3) counterfactual (Bareinboim et al., 2022). A predictive statement, such as “The scene would generate in *this way*,” is a level-1 observational statement. A level-2 interventional statement targets outcomes under hypothetical interventions, such as “If an enemy were placed here (e.g., in a place it would not naturally appear), then the scene would generate in *this way*.” A level-3 counterfactual statement considers observed outcomes and how those outcomes might have been different under hypothetical interventions. For example: “Given there was no enemy and the scene generated that way, if an enemy were placed here, the scene would generate in *this way*.”

Formally, level- k statements describe events in the sample space of a level- k distribution (Bareinboim et al., 2022). Level- k data can be viewed as samples from such a distribution, and with i.i.d. sampling, the empirical distribution converges to the true sampling distribution. Ordinary gameplay logs are level-1 data; data where variables are artificially fixed before sampling (as in experiments) is level-2 data. In most settings, level-3 data does not exist due to the *fundamental problem of causal inference*—it is impossible to observe outcomes for the same effect variables across worlds (Holland, 1986). In this work, we leverage the video game setting’s ability to observe level-3 data across *virtual worlds*, i.e., multiple instances of a game run with shared initial conditions.

Models also align with this hierarchy. A causal DAG is a level-2 model: when combined with a generative model, it encodes the family of interventional distributions over the DAG’s variables. A structural causal model (SCM) is a level-3 model: it additionally encodes the family of counterfactual distributions over the DAG’s variables (Pearl, 2009). Level- k data is sufficient to identify

864 level- k models, but the *causal hierarchy theorem* states that level- k statements cannot, in general,
 865 be inferred from data below level k (Bareinboim et al., 2022).

866 Thus, we follow the three-level hierarchy (Bareinboim et al., 2022): (L1) *observational* questions
 867 about $P(\mathbf{V})$; (L2) *interventional* questions about $P(\mathbf{V} \mid \text{do}(X=x))$; and (L3) *counterfactual*
 868 (parallel-world) questions about joint outcomes under conflicting interventions, e.g.,
 869 $(Y_{X=x}, Y_{X=x'})$. Level-3 quantities encode “all-else-equal” comparisons across worlds.

871 D.2 SCMS AND RULES

872 An SCM $\mathcal{M} = (\mathbf{U}, \mathbf{V}, \mathbf{F}, P(\mathbf{U}))$ specifies exogenous factors \mathbf{U} , endogenous variables \mathbf{V} , structural
 873 assignments \mathbf{F} , and a distribution over \mathbf{U} (Pearl, 2009). In our context, \mathbf{F} plays the role of executable
 874 rules; see Bongers et al. (2018) for SCMs as formal rule systems.

875 D.3 MARGINALIZATION OF CAUSAL DAGS

876 We implement Evans (2016) approach to DAG marginalization. Given a causal DAG and a set of
 877 nodes to marginalize out of the DAG, Evans (2016) creates a marginalized DAG with *hyper-edges*
 878 that represent the footprint of latent common causes. Directed edges encode parent–child relationships
 879 among observed variables as usual. Hyper-edges encompassing a set of observed nodes, indicate
 880 that all nodes in the set share an unobserved exogenous influence. For example, a hyper-edge
 881 touching nodes X, Y, Z represents the fact that there is some unobserved variable that acts as a com-
 882 mon cause to X, Y, Z simultaneously. The mDAG maintains the causal interpretation, intervention
 883 model, and implications to conditional independence as the full DAG.

884 While mDAGs are convenient for reasoning about marginalized structures, we require a fully explicit
 885 DAG representation for generating parallel-world and counterfactual graphs, as well as for using
 886 standard graph serialization. We therefore modify the algorithm such that, for each hyperedge, a
 887 d-separating sets of shared ancestors that entail the hyperedge are explicitly added back into the
 888 model. This implements the expansion of the canonical mDAG by making the latent causes explicit
 889 expansion as discussed in Evans (2016).

890 D.4 MULTIVERSE REASONING.

891 With *multiverse* counterfactual reasoning, we envision one world where observed outcomes oc-
 892 curred, and separate “parallel” worlds where hypothetical interventions lead to outcomes that differ
 893 from the observed outcomes Shpitser & Pearl (2012). For example, consider the statement “Given
 894 there was no enemy and the scene generated *that* way, if an enemy were placed here, the scene
 895 would generate in *this* way”. With this statement, we can envision two parallel worlds, one where
 896 there was no enemy and the scene generated *that* way, and one where there was an enemy and the
 897 scene generated *this* way. Level-3 data, therefore, is a data tuple representing outcomes across par-
 898 allel worlds. The “fundamental problem of causal inference” (Holland, 1986) is that level-3 data
 899 is unobservable—in real world settings, it is impossible to observe potential outcomes for the same
 900 variable across parallel worlds. A key insight of our work is that in *virtual world* settings, the data
 901 can exist by creating parallel instances of the same world with the same initial conditions.

902 D.5 COUNTERFACTUAL GRAPHS AND CONSISTENCY

903 Counterfactual graphs are based on *parallel world graphs*. The parallel world graph clones a causal
 904 DAG across parallel worlds and uses graph surgery to represent hypothetical conditions in certain
 905 worlds (Shpitser & Pearl, 2012). Variables that are *not* descendants of the intervention share a single
 906 node across worlds (consistency); variables affected by the intervention are duplicated and indexed
 907 by world. This graph encodes which quantities must remain identical across worlds and which
 908 may differ, providing a compact template for supervision and evaluation. The counterfactual graph
 909 collapses nodes that must be consistent across worlds into single nodes, creating a graph that (unlike
 910 the parallel world graph) encodes conditional independence across parallel worlds. In this work,
 911 we formalize the concept of game mechanics such that, for a given mechanic, we can generate a
 912 set of parallel world graphs and counterfactual graphs that explicitly encode its structure and which

variables should remain consistent while the mechanic is in play. These can be used in training alongside the level-3 gameplay data.

D.6 ESTIMATING COUNTERFACTUAL DISTRIBUTIONS

In Section 3.1.3, we let $P_1 = P(S_{W=1}, S_{W=0})$, $P_2 = P(B_{S=1}, B_{S=0})$, and $P_3 = P(D_{B=1}, D_{B=0}, S)$ denote the distributions constrained by \mathcal{S}_1 , \mathcal{S}_2 , and \mathcal{S}_3 . We can estimate these distributions with repeated sampling of consistent contrasts \mathcal{D}_1 , \mathcal{D}_2 , and \mathcal{D}_3 , then averaging over sampling distributions to obtain sampling distributions \hat{P}_1 , \hat{P}_2 , and \hat{P}_3 .

- $\hat{P}_1: \sum_{j \in 0,1} \sum_{b_{W=j}^{(i)}, a_{W=j}^{(i)}, v_{W=j}^{(i)}} \hat{P}(S_{W=1}, B_{W=1}, D_{W=1}, V_{W=1}, S_{W=0}, B_{W=0}, D_{W=0}, V_{W=0})$
- $\hat{P}_2: \sum_{j \in 0,1} \sum_{w, d_{S=j}, v_{S=j}} \hat{P}(W, B_{S=1}, D_{S=1}, V_{S=1}, B_{S=0}, D_{S=0}, V_{S=0})$
- $\hat{P}_3: \sum_{j \in 0,1} \sum_{w, s, v_{B=j}} \hat{P}(W, S, D_{B=1}, V_{B=1}, D_{B=0}, V_{B=0})$

In each case \hat{P}_i converges almost surely to P_i .

E MECHANICS IMPLEMENTED IN MULTIVERSE MECHANICA V1.0

In this section, we describe the ground truth causal structure and mechanics Multiverse Mechanica.

We describe each game mechanic in terms of:

- *level-2* interventional statements: A set of causal hypothetical statements of the form “Given preconditions W , all else equal, if X , then Y .”
- A set of causal Markov kernels encompassing the relevant conditional probability distributions in the causal DAG.
- *level-3 parallel world* statements: A set of counterfactual statements of the form “Given preconditions W , all else equal, if X , then Y AND if X' then Y' .”
- A set of counterfactual probability expressions defining the induced counterfactual outcome probabilities.

Particularly, in the case of the level-3 parallel world statements, we can enumerate counterfactual worlds in which we make a change and the target outcome variable(s) change, with guarantees on consistency, with respect to the game mechanic.

We formulate the counterfactual cases by taking interventions to change variables (**bold**), from the factual case (Case 0). Downstream changes are shown in *italics*.

Full Causal DAG Figure 6 shows the full causal DAG of a turn in Multiverse Mechanica v1.0.

E.1 SHIELD MECHANIC

The warrior character can equip a shield they can use to block incoming attacks, if they have a free hand and perform the “defend” action.

E.1.1 LEVEL-2 INTERVENTIONAL DEFINITION

We can completely define this mechanic by a set of contrasting statements:

- If a player has a small weapon, they may hold a shield, otherwise they cannot.
- If a player has a shield, they may block incoming attacks, otherwise they cannot.
- If a player blocks an incoming attack, they avoid taking damage, otherwise they may take damage.

Involved variables:

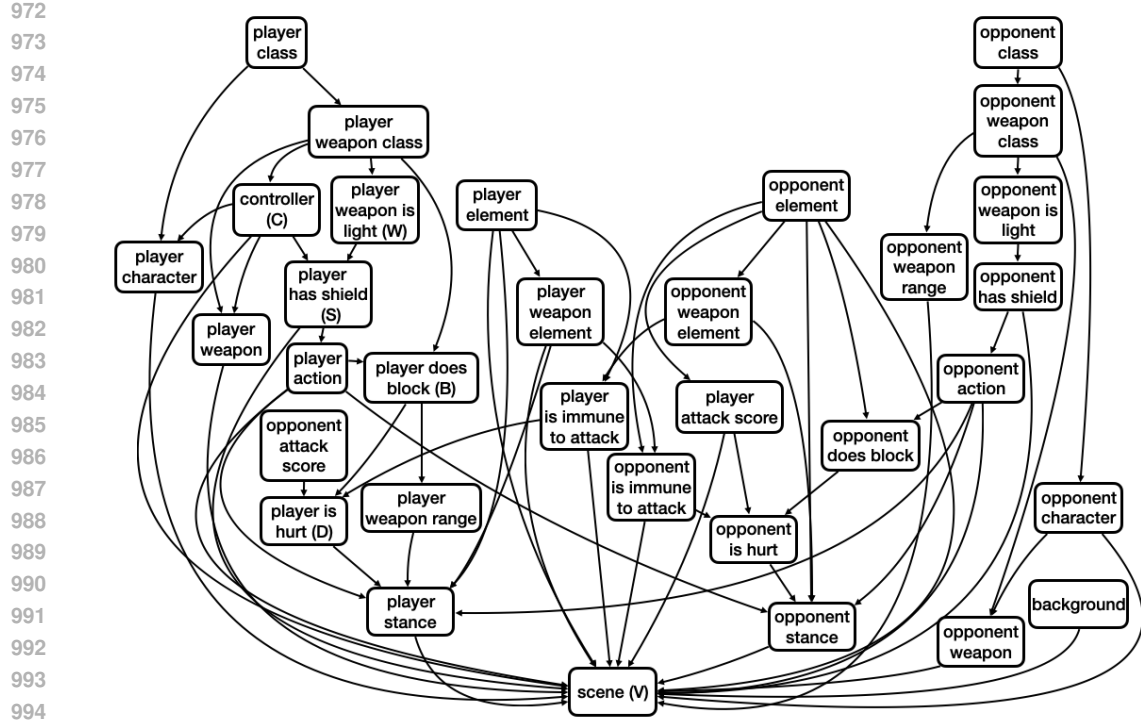
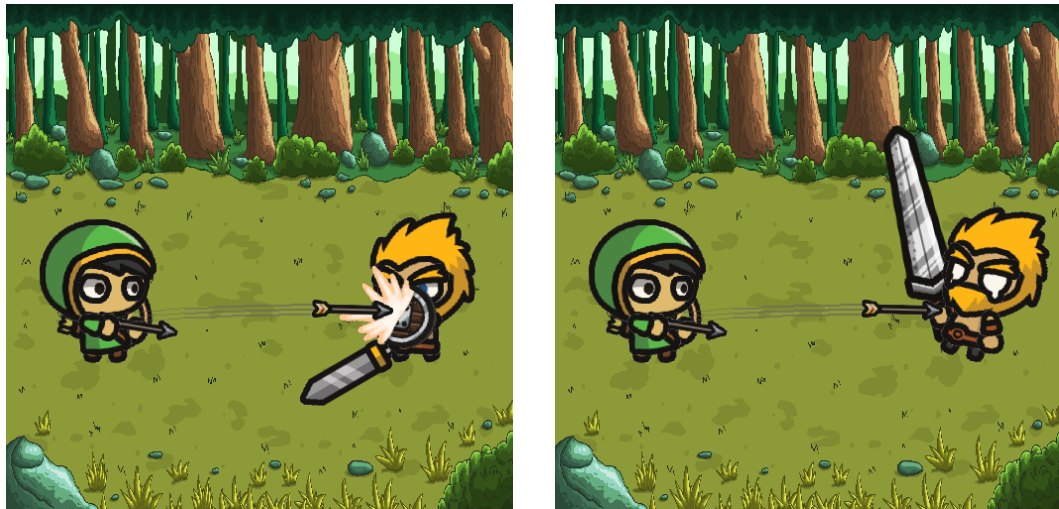


Figure 6: Full causal DAG of a turn in Multiverse Mechanica



(a) Factual: The warrior is equipped with a one-handed short-sword and a shield, and blocks the arrow with a shield.
 (b) Counterfactual: The warrior is equipped with a two-handed long-sword, and no shield, and is unable to block the attack.

Figure 7: Example counterfactual contrast statement for the shield mechanic.

- player action : [idle, melee attack, defend]
- opponent weapon class : [small, large]
- opponent has shield : [True, False]
- opponent action : [idle, melee attack, defend]
- opponent is hurt : [True, False]

1026
1027**Latent variables:**1028
1029

- opponent weapon is heavy : [one-handed, two-handed]

1030
1031

E.1.2 CAUSAL MARKOV KERNELS

1032
1033

In our model, *block* is one of the actions. Thus, we can reason about the shield game mechanic in terms of the player/opponent action being sampled as *block*.

1034

The causal Markov kernel for the opponent action variable encompasses the shield game mechanic:

1035

$$P(\text{opponent action} \mid \text{opponent has shield, opponent weapon}).$$

1036

To reason about the opponent blocking, we consider the probability that the action variable is *block*:

1039

$$P(\text{opponent action} = \text{block} \mid \text{opponent has shield, opponent weapon}).$$

1041
1042
1043

To reason about the opponent getting hurt, we consider the probability that the opponent gets hurt, given the opponent action and player action:

1044
1045

$$P(\text{opponent is hurt} \mid \text{opponent action, opponent has shield, opponent weapon}).$$

1046
1047
1048
1049
1050

An important detail to take note of is that the causal DAG does not have a variable to represent the character’s outcome (e.g. getting hit, blocking, dodging)—it only has a notion of final stance. However, the stance variable is currently unused after sampling; the battle video game handles the underlying outcome logic and renders the scene.

1051
1052
1053
1054

E.1.3 LEVEL-3 COUNTERFACTUAL PARALLEL WORLD STATEMENTS

We can rewrite the level-2 interventional statements as the following level-3 parallel world statements:

1055
1056
1057
1058
1059
1060
1061
1062

- Given a character had a heavy weapon and they did not have a shield; if the character would have had a light weapon instead, then they could have equipped a shield.
- Given a character had not had a shield and did not block; if the character had a shield instead, then they could have blocked.
- Given a character had a shield but did not block and took damage; if the character had blocked instead, then they would have avoided taking damage from the attack.

1063

E.1.4 COUNTERFACTUAL PROBABILITY EXPRESSIONS

1064

We can formulate these natural-language statements in mathematical notation.

1066
1067

Notation. Let:

1068
1069
1070
1071
1072
1073

- WC = weapon class,
- HS = has shield,
- B = does block,
- H = is hurt.

1074
1075

Then we have:

1076
1077
1078
1079

$$P(H_{WC=\text{Light}} = \text{True} \mid WC = \text{Heavy}, HS = \text{False}) > 0,$$

$$P(B_{HS=\text{True}} = \text{True} \mid HS = \text{False}, B = \text{False}) > 0,$$

$$P(H_{B=\text{True}} = \text{False} \mid HS = \text{True}, B = \text{False}, H = \text{True}) = 1.$$

1080
1081

E.2 ELEMENTAL IMMUNITY MECHANIC

1082
1083
1084
1085
1086

Under the elemental immunity game mechanic, players may have elemental attributes; either fire or ice. Weapons may also have elemental attributes. If the attacking player weapon element and opponent element are the same (and non-none), the opponent is granted elemental immunity, and thus avoids taking damage from the attack, since they are already imbued with the element the attacker is using to attack them.

1087

The elemental attributes of characters are indicated by variations from their base appearance:

1088
1089
1090
1091
1092

- *none*: Characters appear in their standard appearances
- *fire*: Characters appear with orange shading and/or red outline
- *ice*: Characters appear with light blue shading and/or blue outline

1093

The elemental attributes of weapons are similarly indicated by variations from their base appearance:

1094

1095

1096

1097

1098

1099

1100

1101

1102

1103
1104
1105
1106
1107
1108
1109
1110
1111
1112
1113
1114
1115
1116
1117
1118
1119

(a) Factual: The fire wizard is immune to the warrior’s melee attack with a fire-type short sword.



(b) Counterfactual: The fire wizard takes damage from the warrior’s melee attack with an ice-type short sword.

1120

1121

1122

1123

1124

1125

1126

Figure 8: Example counterfactual contrast statement for the elemental immunity mechanic.

1127

1128

E.2.1 LEVEL-2 INTERVENTIONAL DEFINITION

1129

1130

1131

1132

1133

We can completely define this mechanic by a set of contrasting statements:

- If a player has an elemental attribute, they may wield a weapon with the same elemental attribute but they cannot wield one of an opposing element in the fire–ice dichotomy. For example, a player with a fire-elemental attribute may wield a fire-elemental weapon (or non-elemental weapon); they cannot wield an ice-elemental weapon.
- If a player does not have an elemental attribute, they may wield any elemental-type weapon; otherwise the rule above applies.

1134 • If a player is hit by an incoming attack from a weapon with the same elemental attribute,
 1135 they are immune and thus avoid taking damage; otherwise they may take damage.
 1136

1137 **Involved variables:**

1138 • player element : [none, fire, ice]
 1139 • player weapon element : [none, fire, ice]
 1140 • opponent element : [none, fire, ice]
 1141 • opponent is immune to attack : [True, False]
 1142 • opponent is hurt : [True, False]
 1143

1144 **Latent variables:** None.

1145 E.2.2 CAUSAL MARKOV KERNELS

1146 The element of the player and the opponent are both independent variables:

1147 $P(\text{player element}),$
 1148 $P(\text{opponent element}).$

1149 The causal Markov kernel for the player weapon elemental is as follows:

1150 $P(\text{player weapon element} \mid \text{player element}).$

1151 To reason about the opponent being immune to the attack, we consider the conditional probability
 1152 given the opponent's element and player's weapon element:

1153 $P(\text{opponent is immune to attack} \mid \text{player weapon element, opponent element}).$

1154 To reason about the opponent getting hurt, we consider the probability that the opponent gets hurt,
 1155 given the opponent being immune:

1156 $P(\text{opponent is hurt} \mid \text{opponent is immune to attack}).$

1157 E.2.3 LEVEL-3 COUNTERFACTUAL PARALLEL WORLD STATEMENTS

1158 We can rewrite the level-2 interventional statements as the following level-3 parallel world state-
 1159 ments:

- 1160 1. Given a character had a fire elemental attribute and they had a fire elemental weapon; if the
 1161 character would have had an ice elemental attribute instead, then they could have had an
 1162 ice- or none-elemental weapon but not a fire elemental.
- 1163 2. Given a character had a fire elemental attribute and they had a fire elemental weapon; if the
 1164 character would have had no elemental attribute instead, then they could have had any
 1165 elemental or non-elemental type weapon.
- 1166 3. Given a character had an ice elemental attribute and was hit with an attack from an ice
 1167 elemental weapon, and thus was immune and did not take damage; if the character had a
 1168 fire elemental attribute instead, then they would have taken damage from the attack.

1169 E.2.4 COUNTERFACTUAL PROBABILITY EXPRESSIONS

1170 We can formulate these natural language statements in mathematical notation.

1171 **Notation.** Let:

1172 • PE = player element,
 1173 • PWE = player weapon element,
 1174 • OE = opponent element,
 1175 • I = is immune to attack,
 1176 • H = is hurt.

1177 Then we have:

1188 **Statement 1.**

1189
$$P(PWE_{PE=\text{Ice}} = \text{Fire} \mid PE = \text{Fire}, PWE = \text{Fire}) = 0,$$

1190
$$P(PWE_{PE=\text{Ice}} = \text{Ice} \mid PE = \text{Fire}, PWE = \text{Fire}) > 0,$$

1191
$$P(PWE_{PE=\text{Ice}} = \text{None} \mid PE = \text{Fire}, PWE = \text{Fire}) > 0.$$

1192

1193 **Statement 2.**

1194
$$P(PWE_{PE=\text{None}} = \text{Fire} \mid PE = \text{Fire}, PWE = \text{Fire}) > 0,$$

1195
$$P(PWE_{PE=\text{None}} = \text{Ice} \mid PE = \text{Fire}, PWE = \text{Fire}) > 0,$$

1196
$$P(PWE_{PE=\text{None}} = \text{None} \mid PE = \text{Fire}, PWE = \text{Fire}) > 0.$$

1197

1198 **Statement 3.**

1199
$$P(H_{OE=\text{Fire}} = \text{True} \mid PWE = \text{Ice}, OE = \text{Ice}) = 1.$$

1200

1201

E.3 WEAPON RANGE MECHANIC

1202 Under the weapon range game mechanic, weapon classes have range attributes; either melee or
1203 ranged. Each weapon class is either a melee or ranged type. For example, the light sword, the
1204 heavy sword, and the dagger are melee weapons; while the bow, the staff, and the throwing knife are
1205 ranged weapons. The weapon range attribute affects primarily visual elements of the battle scene:

1206

1207

1. **Stance:** a character attacking with a melee weapon will be depicted in the snapshot physically
1208 swinging the melee weapon at the opponent’s location, while a character attacking with a ranged weapon will be depicted shooting/throwing/casting from their position.

1209 2. **Scene:** a character attacking with a melee weapon will be shown in the game scene (video) first
1210 approaching the opponent’s position before physically swinging the melee weapon, while a character attacking with a ranged weapon will be depicted shooting/throwing/
1211 casting from their position and the emitted projectile will be shown traveling towards the
1212 opponent from left to right (possibly on a parabolic trajectory, if affected by gravity, e.g.
1213 the arrow shot from the bow).

1215 (a) Factual: The assassin performs a melee attack on
1216 a wizard with a sword.1218 (b) Counterfactual: The assassin performs a ranged
1219 attack on a wizard with a throwing knife.

1220

1221

1222

1223

1224

1225

1226

1227

1228

1229

1230

1231

1232

1233

1234

1235

1236

1237

1238

1239

1240

1241

Figure 9: Example counterfactual contrast statement for the weapon range mechanic.

1242 E.3.1 LEVEL-2 INTERVENTIONAL DEFINITION
 1243
 1244 We can completely define this mechanic by a set of contrasting statements:
 1245
 1246 • If a weapon is one of the weapon classes *light sword*, *heavy sword*, or *dagger*, it is a melee
 1247 weapon; otherwise if it is *bow*, *staff*, or *throwing knife* it is a ranged weapon.
 1248 • If a player wields a melee weapon, they will be depicted in the snapshot as performing a
 1249 melee attack at the opponent’s location; otherwise they will be depicted as performing a
 1250 ranged attack from their own location.
 1251 • If a player wields a melee weapon, they will be shown in the game scene (video) first
 1252 approaching the opponent’s position before physically swinging the melee weapon; other-
 1253 wise they will be depicted shooting/throwing/casting from their position and the emitted
 1254 projectile will be shown traveling towards the opponent from left to right.

1255 **Involved variables:**
 1256

1257 • player weapon class : [light sword, heavy sword, dagger, bow, staff, throwing
 1258 knife]
 1259 • player weapon range : [melee, ranged]
 1260 • player stance : pixels in the rendered image snapshot
 1261 • scene : pixels in the rendered gameplay video
 1262

1263 **Latent variables:** None.
 1264

1265 E.3.2 CAUSAL MARKOV KERNELS
 1266

1267 The causal Markov kernel for the player weapon range is as follows:

$$P(\text{player weapon range} \mid \text{player weapon class}).$$

1270 To reason about the player stance rendered in the image snapshot, we consider the conditional prob-
 1271 ability given the player weapon and player weapon range:

$$P(\text{stance} \mid \text{player weapon, player weapon range}).$$

1274 Similarly, to reason about the scene rendered in the gameplay video, we consider the conditional probability given the player weapon, player weapon range, and player stance:

$$P(\text{scene} \mid \text{player weapon, player weapon range, stance}).$$

1278 E.3.3 LEVEL-3 COUNTERFACTUAL PARALLEL WORLD STATEMENTS
 1279

1280 We can rewrite the level-2 interventional statements as the following level-3 parallel world state-
 1281 ments:

1. Given a character had a light sword and they had a melee weapon; if the character would have had a bow instead, then they would have had a ranged weapon.
2. Given a character had a melee weapon and they were depicted in the snapshot as performing a melee attack at the opponent’s location; if the character would have had a ranged weapon instead, then they would have been depicted as performing a ranged attack from their own location.
3. Given a character had a melee weapon and they were shown in the game scene video first approaching the opponent’s position before physically swinging the melee weapon; if the character would have had a ranged weapon instead, then they would have been depicted shooting/throwing/casting from their position and the emitted projectile would have been shown traveling towards the opponent from left to right.

1294 E.3.4 COUNTERFACTUAL PROBABILITY EXPRESSIONS
 1295

We can formulate these natural language statements in mathematical notation.

1296

Notation. Let:

1297

1298

1299

1300

1301

1302

1303

1304

1305

1306

1307

- PWC = player weapon class,
- PWR = player weapon range,
- PS = player stance,
- S = scene.

1308 Then we have:

1309

Statement 1.

1310

1311

1312

1313

1314

1315

1316

1317

$$P(PWR_{PWC=\text{bow}} = \text{ranged} \mid PWC = \text{light sword}, PWR = \text{melee}) = 1.$$

Statement 2.

1318

1319

1320

1321

1322

1323

1324

1325

1326

1327

1328

1329

1330

1331

1332

1333

1334

1335

1336

1337

$$P(PS_{PWR=\text{ranged}} = \text{depicted performing ranged attack} \mid PWR = \text{melee}, PS = \text{depicted performing melee attack}) = 1, \quad (1)$$

$$P(PS_{PWR=\text{ranged}} = \text{depicted performing melee attack} \mid PWR = \text{melee}, PS = \text{depicted performing melee attack}) = 0. \quad (2)$$

Statement 3.

$$P(S_{PWR=\text{ranged}} = \text{shown performing ranged attack} \mid PWR = \text{melee}, PS = \text{shown approaching the opponent and performing melee attack}) = 1, \quad (3)$$

$$P(S_{PWR=\text{ranged}} = \text{shown performing melee attack} \mid PWR = \text{melee}, PS = \text{shown approaching the opponent and performing melee attack}) = 0. \quad (4)$$

E.4 SPELL-CASTING MECHANIC

Under the spell-casting mechanic, the wizard character may perform one of five spells:

1332

1333

1334

1335

1336

1337

1. **Spawn Magic Projectile Spell to Perform Ranged Attack**
2. **Summon Cloud Platform Spell to Dodge Attack**
3. **Self-Transform Spell to Increase Melee Strength**
4. **Opponent Transform Spell to Lower Enemy Defense**
5. **Levitation Spell to Disarm Opponent**

1338

1339

1340

1341

1342

1343

1344

1345

1346

1347

1348

1349

None of these spell actions can be mitigated by the enemy. Even in the case of the self-transform spell, the sheer size of the transformed wizard (into a golem) renders any block action by the opponent useless. Each spell action choice affects the *stance* and *scene* variables in the rendered game.

E.4.1 LEVEL-2 INTERVENTIONAL DEFINITION.

All spells share the same base level-2 contrasting statements:

- If the player character is a wizard, they may wield a magical staff, otherwise they cannot.
- If the character is equipped with a magical staff, they may cast spells, otherwise they cannot.
- If the character casts a spell, they gain a particular offensive or defensive benefit to help them in the battle, otherwise they do not.

1350 E.4.2 CAUSAL MARKOV KERNELS
 1351
 1352 **Notation.** Let:
 1353 • PC = player character
 1354 • PW = player weapon
 1355 • PA = player action
 1356 • PF = player form
 1357 • PS = player stance
 1358 • OC = opponent character
 1359 • OW = opponent weapon
 1360 • OA = opponent action (e.g., defend)
 1361 • OF = opponent form
 1362 • OS = opponent stance
 1363 • B = opponent successfully blocks (semantic variable, only true if the defend action actually succeeds)
 1364 • D = opponent dodges
 1365 • H = opponent is hurt
 1366 • Stance and Scene are the rendered variables
 1367
 1368
 1369
 1370
 1371
 1372 **Latent variables:**
 1373
 1374 • OIA = opponent incoming attack indicator
 1375
 1376 **Shared enabling kernels.**
 1377 $P(PW = \text{staff} \mid PC = \text{wizard}) > 0$
 1378
 1379 $P(PA \in \{\text{spell actions}\} \mid PW \neq \text{staff}) = 0$
 1380 $P(PA \mid PW = \text{staff, state})$ is exogenous (agent policy)
 1381
 1382 **Shared state & rendering kernels.**
 1383 $P(PF, PS, OF, OS \mid PA, OA, PC, PW, OC, OW)$
 1384
 1385 $P(\text{Stance} \mid PF, PS, OF, OS, PA, OA)$
 1386 $P(\text{Scene} \mid \text{Stance}, PF, PS, OF, OS, PA, OA)$
 1387
 1388 **Shared interaction/outcome kernels.**
 1389 $P(B \mid PF, OA)$
 1390
 1391 $P(D \mid PS, OIA)$
 1392
 1393 $P(H \mid B, D, PA)$
 1394
 1395 E.4.3 LEVEL-3 COUNTERFACTUAL PARALLEL WORLD STATEMENTS.
 1396
 1397 All spells also share a common set of counterfactual statements:
 1398 1. Given a character was not a wizard and therefore could not wield a magical staff; if the character had been a wizard instead, then they could have wielded a magical staff.
 1399
 1400 2. Given a character was not equipped with a magical staff and therefore could not cast spells; if the character had been equipped with a staff instead, then they could have cast spells.
 1401
 1402 3. Given a character did not cast a spell and therefore received no benefit in the battle; if the character had cast a spell instead, then they would have gained the corresponding offensive or defensive benefit.
 1403

1404 E.4.4 COUNTERFACTUAL PROBABILITY EXPRESSIONS (SHARED).
1405
1406
14071408 *Not wizard* \rightarrow *Wizard* \Rightarrow *Staff access*
1409

1410
$$P(PW_{PC=\text{wizard}} = \text{staff} \mid PC \neq \text{wizard}, PW \neq \text{staff}) > 0.$$

1411

1412 *No staff* \rightarrow *Staff* \Rightarrow *Spell casting possible*
1413

1414
$$P(PA_{PW=\text{staff}} \in \{\text{spell actions}\} \mid PW \neq \text{staff}, PA \notin \{\text{spell actions}\}) > 0.$$

1415

1416 E.5 SPAWN MAGIC PROJECTILE SPELL TO PERFORM RANGED ATTACK
14171418 The wizard can cast a spell to conjure and launch a magical projectile directly at the opponent. This
1419 action is a ranged attack, and its visual and mechanical dynamics follow the same principles as other
1420 ranged weapons described in Section E.3.
14211422 E.5.1 LEVEL-2 INTERVENTIONAL DEFINITION.
14231424

- If the wizard casts the spawn projectile spell, a magical projectile is launched towards the
opponent (i.e., $OIA = \text{True}$), otherwise no projectile is spawned ($OIA = \text{False}$).
- If a magical projectile strikes the opponent and is not successfully blocked or dodged, the
opponent is hurt, otherwise they are not.

14271428 **Involved variables:**
14291430

- PA = player action
- OA = opponent action (e.g., defend, dodge)
- PS = player stance
- B = opponent successfully blocks
- D = opponent dodges
- H = opponent is hurt

14381439 **Latent variables:**
14401441

- OIA = opponent incoming attack indicator

14421443 E.5.2 CAUSAL MARKOV KERNELS.
1444

1445
$$P(OIA \mid PA)$$

1446

1447
$$P(B \mid PF, OA)$$

1448

1449
$$P(D \mid PS, OIA)$$

1450

1451
$$P(H \mid B, D, PA)$$

1452

E.5.3 LEVEL-3 COUNTERFACTUAL PARALLEL WORLD STATEMENTS.
14531454

1. Given the wizard idled and there was no incoming attack; if the wizard had cast the spawn
projectile spell instead, then the opponent would have faced an incoming attack ($OIA =$
 True).
2. Given the wizard cast the spawn projectile spell and the projectile hit (i.e., no successful
block or dodge) and the opponent was hurt; if the opponent had successfully blocked or
dodged instead, then they would not have been hurt.

1455

1458 E.5.4 COUNTERFACTUAL PROBABILITY EXPRESSIONS.

1459

1460

1461

1462

Idle \rightarrow *Projectile spell* \Rightarrow *Incoming attack present*

1463

$$P(OIA_{PA=\text{projectile spell}} = \text{True} \mid PA = \text{idle}, OIA = \text{False}) = 1.$$

1464

1465

Projectile hits \rightarrow *Successful block* \Rightarrow *Not hurt*

1466

1467

$$P(H_{B=\text{True}} = \text{False} \mid PA = \text{projectile spell}, OIA = \text{True}, B = \text{False}, H = \text{True}) = 1.$$

1468

Projectile hits \rightarrow *Successful dodge* \Rightarrow *Not hurt*

1469

1470

$$P(H_{D=\text{True}} = \text{False} \mid PA = \text{projectile spell}, OIA = \text{True}, D = \text{False}, H = \text{True}) = 1.$$

1471

E.5.5 SUMMON CLOUD PLATFORM SPELL TO DODGE ATTACK

1472

1473

The wizard has a spell they can use to summon a levitating cloud platform and use it to raise themselves up above the battlefield to dodge incoming enemy attacks.

1474

1475

level-2 Interventional Definition.

1476

1477

- If the wizard casts the cloud platform spell, a platform is summoned; the wizard moves onto it and is levitated upwards above the battlefield, otherwise they remain on the ground.
- If the wizard is in an elevated position on a platform during an incoming attack, they successfully dodge and avoid damage, otherwise if they are on the ground they remain vulnerable and may take damage.

1478

1479

1480

1481

1482

Involved variables:

1483

1484

1485

1486

1487

1488

1489

- PA = player action
- OA = opponent action
- OS = opponent stance (grounded, elevated)
- H = opponent is hurt

1490

Latent variables: None.

1491

1492

Causal Markov Kernels.

1493

1494

1495

1496

$$\begin{aligned} P(OS \mid PA) \\ P(D \mid OS, OIA), \\ P(H \mid D). \end{aligned}$$

1497

level-3 Counterfactual Parallel World Statements.

1498

1499

1500

1501

1502

1503

1. Given the wizard performed the idle action and remained on the ground; if the wizard had cast the cloud platform spell instead, then they would have been elevated.
2. Given the wizard remained on the ground during an incoming attack and was hurt; if the wizard had cast the cloud platform spell instead, then they would have been elevated and dodged the attack, and thus not been hurt.

1504

1505

Counterfactual Probability Expressions.

1506

1507

Idle \rightarrow *Cloud Platform* \Rightarrow *Elevated stance*

1508

1509

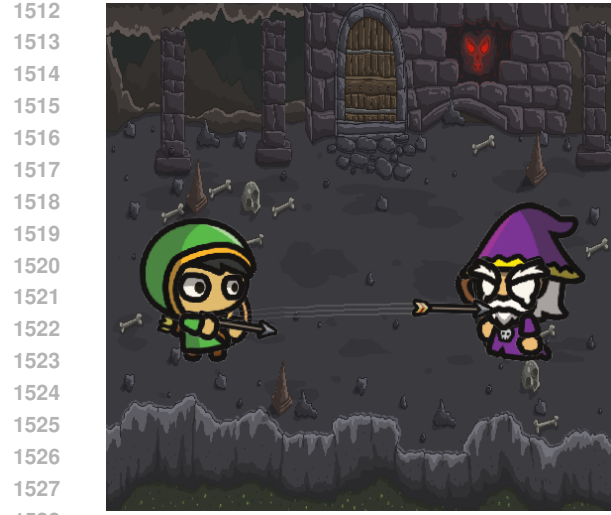
$$P(OS_{PA=\text{cloud platform}} = \text{elevated} \mid PA = \text{idle}, OS = \text{grounded}) = 1.$$

1510

Grounded, hurt during incoming attack \rightarrow *Cloud Platform* \Rightarrow *Dodge, not hurt*

1511

$$P(H_{OS=\text{elevated}} = \text{False} \mid PA = \text{idle}, OS = \text{grounded}, OIA = \text{True}, H = \text{True}) = 1.$$



1512
1513
1514
1515
1516
1517
1518
1519
1520
1521
1522
1523
1524
1525
1526
1527
1528
1529
1530
1531
1532
1533
1534
1535
1536
1537
1538
1539
1540
1541
1542
1543
1544
1545
1546
1547
1548
1549
1550
1551
1552
1553
1554
1555
1556
1557
1558
1559
1560
1561
1562
1563
1564
1565
(a) Factual: The wizard idles and is struck by the archer's arrow.



(b) Counterfactual: The wizard summons a magical cloud platform to gain an elevated position and dodge the archer's arrow.

Figure 10: Example counterfactual contrast statement for the summon cloud platform spell mechanic.

E.5.6 SELF-TRANSFORM SPELL TO INCREASE MELEE STRENGTH

The wizard can cast a spell to transform themselves into a large golem. In this form, their melee attacks are enormously strengthened and cannot be blocked by opponents.

level-2 Interventional Definition.

- If the wizard casts the self-transform spell, they transform into a golem, otherwise they remain in their normal form.
- If the wizard is transformed into a golem, their melee attack cannot be blocked due to sheer size and strength, otherwise it can.
- If the wizard's golem-form melee attack is not successfully blocked, the opponent will be hurt, otherwise they will not be.

Involved variables:

- PA = player action
- OA = opponent action (e.g., defend)
- B = opponent successfully blocks
- H = opponent is hurt

Latent variables:

- PF = player form (normal, golem)

Causal Markov Kernels.

$$P(PF | PA)$$

$$P(B | PF, OA)$$

$$P(H | B, PA)$$

1566
1567**level-3 Counterfactual Parallel World Statements.**1568
1569
1570

- Given the wizard performed the idle action and their form remained unchanged; if the wizard had cast the self-transform spell instead, then they would have transformed into a mighty golem.
- Given the wizard cast a projectile spell and it was blocked by the opponent; if the wizard had cast the self-transform spell instead, then they would have transformed into a golem and the melee attack would not have been blocked by the opponent.
- Given the wizard cast a projectile spell and it was blocked by the opponent and thus they were not hurt; if the wizard had cast the self-transform spell instead, then they would have transformed into a golem and the melee attack would have bypassed the block and hurt the opponent.

1571
1572
15731574
1575
1576
1577
1578**Counterfactual Probability Expressions.**

1579

1580

Idle → Self-Transform ⇒ Golem form

1581

1582

$$P(PF_{PA=\text{self-transform}} = \text{golem} \mid PA = \text{idle}, PF = \text{normal}) = 1.$$

1583

1584

Magic projectile attack blocked → Self-Transform ⇒ Block attempt failed

1585

1586

$$P(B_{PF=\text{golem}} = \text{True} \mid PA = \text{magic projectile attack}, PF = \text{normal}, OA = \text{defend}, B = \text{True}) = 0.$$

1587

1588

Magic projectile attack blocked, not hurt → Self-Transform ⇒ Hurt despite block action

1589

1590

$$P(H_{PF=\text{golem}} = \text{True} \mid PA = \text{magic projectile attack}, PF = \text{normal}, OA = \text{defend}, H = \text{False}) = 1.$$

1591

1592



1593

1594



1595

1596

1597

1598

1599

1600

1601

1602

1603

1604

1605

1606

1607

1608

1609

1610

(a) Factual: The wizard casts a magic projectile spell but the warrior blocks it.

(b) Counterfactual: The wizard casts a spell to transform itself into a large golem to perform a powerful melee attack.

1611

1612

1613

1614

1615

1616

1617

1618

1619

Figure 11: Example counterfactual contrast statement for the self-transform spell mechanic.

E.5.7 OPPONENT TRANSFORM SPELL TO LOWER ENEMY DEFENSE

The wizard can cast a spell to transform an opponent into a weak or harmless creature (i.e., a snail), disarming them and preventing them from defending against incoming attacks.

1620

level-2 Interventional Definition.

1621

1622

- If the wizard casts no spell, the opponent retains their normal form and can block or defend as usual.
- If the wizard casts the opponent transform spell, the opponent is transformed (e.g. into a snail), otherwise they remain in their normal form.
- If the opponent is transformed, they are disarmed and cannot block; otherwise they may block.

1623

1624

1625

1626

1627

1628

1629

Involved variables:

1630

1631

1632

1633

1634

1635

1636

Latent variables:

1637

1638

1639

1640

Causal Markov Kernels.

1641

1642

1643

$$P(OF \mid PA),$$

$$P(H \mid OF, B).$$

1644

level-3 Counterfactual Parallel World Statements.

1645

1646

1647

1648

1649

1650

1651

1652

1. Given the wizard cast a projectile spell and the opponent remained in their normal form; if the wizard had cast the opponent transform spell instead, then the opponent would have been transformed into a snail.
2. Given the wizard cast a projectile spell and it was blocked by the opponent, and thus the opponent was not hurt; if the wizard had cast the opponent transform spell instead, then the opponent would have been unable to block and would have been hurt by a follow-up attack.

1653

Counterfactual Probability Expressions.

1654

1655

1656

Idle or projectile spell \rightarrow Opponent Transform \Rightarrow Opponent form changes

1657

1658

$$P(OF_{PA=\text{opponent transform}} = \text{transformed} \mid PA \neq \text{opponent transform}, OF = \text{normal}) = 1.$$

1659

Projectile spell blocked, not hurt \rightarrow Opponent Transform \Rightarrow Block disabled (opponent disarmed)

1660

1661

1662

$$P(B_{OF=\text{transformed}} = \text{True} \mid PA = \text{magic projectile attack}, OF = \text{normal}, B = \text{True}) = 0.$$

1663

E.5.8 LEVITATION SPELL TO DISARM OPPONENT

1664

1665

1666

The wizard can cast a spell that lifts the opponent into the air, leaving them unable to defend or block effectively, and rendering them disarmed.

1667

1668

level-2 Interventional Definition.

1669

1670

1671

1672

1673

- If the wizard casts no spell, the opponent remains grounded and may block normally.
- If the wizard casts the levitation spell, the opponent is lifted into the air, otherwise they remain grounded.
- If the opponent is levitated, they cannot block and are effectively disarmed; otherwise they may block.



(a) Factual: The wizard casts a magic projectile spell but the warrior blocks it.



(b) Counterfactual: The wizard casts a spell to transform the warrior into a snail to disarm them.

Figure 12: Example counterfactual contrast statement for the opponent transform spell mechanic.

Involved variables:

- PA = player action
- OA = opponent action
- OS = opponent stance (grounded, levitating)
- B = opponent successfully blocks
- H = opponent is hurt

Latent variables: None.

Causal Markov Kernels.

$$P(OS \mid PA),$$

$$P(H \mid OS, B)$$

level-3 Counterfactual Parallel World Statements.

- Given the wizard cast a projectile spell and the opponent remained grounded; if the wizard had cast the levitation spell instead, then the opponent would have been levitated.
- Given the wizard cast a projectile spell and it was blocked by the opponent, and thus the opponent was not hurt; if the wizard had cast the levitation spell instead, then the opponent would have been unable to block and left vulnerable.

Counterfactual Probability Expressions.

Idle or projectile spell → Levitation ⇒ Opponent stance changes

$$P(OS_{PA=\text{levitation}} = \text{levitating} \mid PA \neq \text{levitation}, OS = \text{grounded}) = 1.$$

Projectile spell blocked, not hurt → Levitation ⇒ Block disabled (opponent disarmed)

$$P(B_{OS-\text{levitating}} \equiv \text{True} \mid PA \equiv \text{magic projectile attack}, OS \equiv \text{grounded}, B \equiv \text{True}) \equiv 0.$$



1728
1729
1730
1731
1732
1733
1734
1735
1736
1737
1738
1739
1740
1741
1742
1743
1744
1745
1746
(a) Factual: The wizard casts a magic projectile spell
but the warrior blocks it.



1744
1745
1746
1747
1748
1749
1750
1751
1752
1753
1754
1755
1756
1757
1758
1759
1760
1761
1762
1763
1764
1765
1766
1767
1768
1769
1770
1771
1772
1773
1774
1775
1776
1777
1778
1779
1780
1781
(b) Counterfactual: The wizard casts a levitation spell
to lift the warrior off the ground, disarming them.

Figure 13: Example counterfactual contrast statement for the levitation spell mechanic.

F GAME DESIGN DECISIONS

To ensure that the datasets produced by our simulation respect the causal assumptions of our model, we designed the game architecture with consistency guarantees as a primary objective. This appendix documents how these guarantees were realized in practice, focusing on two complementary aspects: (i) the modular, system-based design of game mechanics that mirrors the structure of the causal model, and (ii) the temporal alignment of captured frames to ensure semantic consistency in dynamic interactions.

F.1 BRIDGING GAME MECHANICS AND CAUSAL MECHANISMS WITH SYSTEM-BASED DESIGN

At the foundation of our data generation pipeline lies a design principle: game mechanics must be implemented in a way that respects and preserves the structure of the causal model they instantiate. To achieve this, we adopted a fully modular *Entity–Component–System* (ECS) architecture (Nystrom, 2014; Gregory, 2018), which enforces locality of causal mechanisms and supports reproducibility across runs.

F.1.1 ENTITIES, COMPONENTS, AND SYSTEMS AS CAUSAL UNITS.

In our implementation, *entities* represent the units of analysis (e.g., characters, projectiles, platforms), *components* represent their attributes and state (e.g., position, animation phase, shield presence), and *systems* encapsulate the transformation rules that govern state evolution (e.g., combat resolution, kinematics, physics, or screenshot scheduling). This separation guarantees that each causal mechanism is expressed locally, without entanglement with unrelated processes.

Each system implements a distinct causal mechanism: for example, the *GameCombatSystem* maps action states of attacker and defender into outcomes such as *hit*, *block*, or *immune*, while the *GamePhysicsSystem* governs the motion of projectiles according to deterministic physical rules. Systems are generally designed to operate frame-by-frame using component data as inputs, but they may also maintain local state when required (for example, the *GameAnimationSystem* manages a per-entity priority queue of animation requests). This design ensures that each causal transformation is encapsulated and modular, while still supporting the persistent state needed for realistic simulation.

1782 F.1.2 ALIGNMENT WITH CAUSAL GRAPH STRUCTURE
1783

1784 The ECS architecture was chosen deliberately to reflect the modular structure of our causal model.
1785 Nodes in the causal graph correspond to entity attributes (e.g., *weapon class*, *stance*, *elemental*
1786 *immunity*), while edges correspond to the update dependencies realized through system logic.

1787 For example, the transition of a defender into a *blocking* or *hurt* state depends on multiple up-
1788 stream components: the presence of a shield component, the character’s action selection com-
1789 ponent (indicating whether the chosen action is to block), and downstream trigger flags such as
1790 `needs_to_block` or `is_hurt`. The shield and action selection components establish the poten-
1791 tial for blocking, while the trigger flags are set based on situational context (e.g., proximity of an
1792 incoming attack). Only when both preconditions and triggers align does the GameCombatSystem
1793 update the defender’s state to *blocking*; otherwise, the state transitions to *hurt*.

1794 This design directly encodes the causal mechanism:

1795 shield component + action selection $\rightarrow \{\text{needs_to_block}, \text{is_hurt}\} \rightarrow$ outcome (block or hurt).
1796

1797 By structuring dependencies in this way, the system preserves the logic of the causal graph within the
1798 mechanics of the game engine. This mapping ensures that system update rules correspond closely
1799 to the assignment functions of the causal model.
1800

1801 F.1.3 LOCALITY AND MODULARITY FOR CONSISTENCY
1802

1803 By localizing mechanics in dedicated systems, the architecture prevents hidden confounding
1804 across game features. For instance, animation timing is managed exclusively by
1805 the GameAnimationSystem, while collision and trajectory updates are confined to the
1806 GamePhysicsSystem. This guarantees that modifying one mechanism (e.g., projectile grav-
1807 ity) does not inadvertently alter another (e.g., collision detection or blocking). Such modularity
1808 enforces a form of “causal isolation,” allowing dataset generation to reflect the true structure of the
1809 designed model.

1810 F.1.4 REPRODUCIBILITY AND CONNECTION TO INTERVENTIONS
1811

1812 The ECS structure also guarantees reproducibility: since each system applies deterministic update
1813 rules to the current component state, identical initial conditions yield identical traces. Importantly,
1814 the systems themselves do not support interventions in the sense of directly overriding assignment
1815 functions during simulation. Instead, interventions are handled at the model level: sampled val-
1816 ues from the causal model are passed into the simulation as inputs that determine which branches
1817 of the GameBehaviorTree are executed (e.g., sampled values specifying whether a character
1818 *does block*). The behavior tree then orchestrates the scene by triggering the appropriate system up-
1819 dates, while each system executes its assignment function deterministically given the requested state
1820 changes. In this way, the game engine acts as a faithful executor of causal mechanisms, while the
1821 intervention logic is confined to the sampling layer above.

1822 Through this design, the simulation environment operates as a direct computational analogue of
1823 the causal model, where each mechanism is encapsulated in a corresponding system. This guaran-
1824 tees that generated training data inherits the same modularity and independence properties as the
1825 underlying causal graph, thereby supporting consistency-guaranteed counterfactual analysis.
1826

1827 F.2 IMPACT FRAMES: DEFINING SEMANTIC CONSISTENCY IN DYNAMIC CAUSAL MODEL
1828 TRACES VIA *Point of Maximum Action* CONCEPT
1829

1830 While the system-based architecture guarantees local causal consistency at the level of game logic,
1831 temporal alignment must also be addressed to preserve counterfactual consistency in dynamic inter-
1832 actions. To this end, our system generates gameplay clips of contrasting player turns, each designed
1833 to include a canonical *impact frame*: the instant an attack connects, a shield block occurs, or a projec-
1834 tile visibly misses. Ensuring that these per-turn impact frames correspond to semantically equivalent
1835 points in the causal process is critical; otherwise, contrasts risk reflecting phase misalignment rather
than true causal differences. We therefore formalize alignment using the *Point of Maximum Action*

1836 (PoMA) principle, which anchors impact frames to the most visually and mechanically expressive
 1837 phase of the interaction.
 1838

1839 **F.2.1 CONCEPTUAL FRAMING: TEMPORAL ALIGNMENT FOR COUNTERFACTUAL
 1840 COMPARISONS**

1842 In static structural causal models (SCMs), counterfactuals are evaluated at a single time index, and
 1843 semantic alignment across factual and counterfactual worlds is immediate. In dynamic SCMs, the
 1844 meaning of an event depends on *when* it occurs relative to the unfolding process. For example, a
 1845 melee strike might connect later than a projectile impact due to differences in action duration. If
 1846 frames are extracted at fixed indices, we risk capturing non-equivalent phases of these interactions
 1847 (e.g., an attack wind-up in one turn versus a point of contact in another). If we extract training
 1848 artifacts (e.g., impact frames) at fixed indices, we risk capturing non-equivalent phases of these
 1849 interactions (such as a wind-up in one run versus a point of contact in another). This undermines
 1850 the validity of counterfactual comparisons by introducing differences that are artifacts of temporal
 1851 phasing rather than consequences of the intervention.

1852 We therefore treat each player turn as a temporal *causal trace* and align counterfactual observa-
 1853 tions to the *most informative temporal locus* of the relevant event class. We formalize this with the
 1854 principle of the *Point of Maximum Action* (PoMA).

1855 **F.2.2 POINT OF MAXIMUM ACTION (POMA).**

1856 Let $A(S_{t'}) \in \mathbb{R}_{\geq 0}$ score how *action-intense* the counterfactual state $S_{t'}$ is with respect to the target
 1857 event class (e.g., impact, block). The PoMA alignment selects

$$t'_{\text{PoMA}} = \arg \max_{t' \in T'} A(S_{t'}).$$

1859 PoMA frames are then extracted at t'_{PoMA} , aligning the impact frame to the point of maximum
 1860 expressivity. This guarantees that contrasts correspond to the same semantic phase of the interaction,
 1861 regardless of variation in action duration.

1862 **F.2.3 FOUR ALIGNMENT METHODS: BRIEF SUMMARY WITH PROS AND CONS**

1863 We summarize four practical approaches for temporal alignment of dynamic counterfactuals. Each
 1864 provides a distinct trade-off between simplicity, robustness, and semantic fidelity.

1865 **1) Constant Time Interval.** *Rule.* Evaluate the counterfactual variable at the same nominal time
 1866 as the factual: $t' \equiv t$. *Pros.* Conceptually simple; trivial to implement; deterministic. *Cons.* Fails
 1867 when action durations differ; risks capturing non-equivalent phases (e.g., mid-swing vs. impact);
 1868 unsuitable for dynamic interactions where event timing adapts to interventions.

1869 **2) Equilibrium-Based.** *Rule.* Evaluate once the counterfactual dynamics have reached a steady state
 1870 or absorbing condition (e.g., $\|S'_{t'+1} - S'_{t'}\| < \varepsilon$ or a domain predicate holds). *Pros.* Appropriate for
 1871 tasks where long-run properties matter; robust to transient phasing differences; alignment invariant
 1872 to small shifts in sequence length. *Cons.* Inapplicable to inherently transient events (e.g., impacts);
 1873 some episodes may not converge; equilibrium may erase the very distinctions needed to analyze
 1874 acute causal effects.

1875 **3) Point of Maximum Action (PoMA).** *Rule.* Align to the counterfactual time of peak action
 1876 intensity for the event class:

$$t'_{\text{PoMA}} = \arg \max_{t'} A(S'_{t'}).$$

1877 *Pros.* Directly targets the most salient phase of the interaction; robust to differences in sequence
 1878 length; naturally accommodates variable-duration actions by abstracting to their peak. *Cons.* Re-
 1879 quires a well-defined intensity score A ; can be non-trivial for abstract or multi-agent interactions;
 1880 may require smoothing when peaks are brief or noisy.

1881 **4) Semantic Consistency.** *Rule.* Align by maximizing semantic similarity between factual and
 1882 counterfactual states. *Pros.* General and flexible in principle; useful in settings where semantic
 1883 descriptors are available. *Cons.* Not used in our implementation. It requires an additional similarity
 1884 metric and embedding design, which introduces complexity and potential bias.

1890 In practice, we adopt the PoMA approach, extending it with event-specific scoring functions and
 1891 event-defined windows to handle variable-duration interactions. Constant Time and Equilibrium
 1892 serve primarily as conceptual baselines, while semantic similarity was considered but not imple-
 1893 mented.
 1894

1895 **F.2.4 IMPLEMENTATION IN OUR GAME: EVENT-BASED WINDOWS AND WEIGHTED
 1896 SCORING**

1897 To instantiate these principles in a reproducible data pipeline, our engine implements an event-driven
 1898 *GameScreenshotSystem* that schedules captures at semantically aligned moments:
 1899

1900 1. **Event Detection.** The simulation raises structured events for interactions of interest (e.g.,
 1901 `melee_impact`, `projectile.hit`, `shield.block`). Each event is associated with
 1902 the participating entities and their current states.
 1903 2. **Event-Based Scoring Windows.** For each interaction type, we define a start event
 1904 and a stop event that bound a scoring window (e.g., `swing_start` → `impact`, or
 1905 `projectile.cast` → `collision`). These windows are managed directly in the be-
 1906 havior tree, ensuring that scoring only occurs during the semantically relevant phase of the
 1907 interaction.
 1908 3. **Weighted Scoring.** Within each window, frames are scored according to event-specific
 1909 weights. For example, projectile impact events may be given higher weight than projectile
 1910 flight, and shield contact may be prioritized over shield raise. The capture frame is then
 1911 chosen as

$$\hat{t}' \in \arg \max_{t' \in \text{window}} A(S'_{t'}),$$

1914 with deterministic tie-breaking for reproducibility.
 1915

1916 By anchoring artifact capture to event-defined scoring windows and applying weighted intensity
 1917 scoring, our pipeline produces semantically aligned visual data across simulations, despite natu-
 1918 ral variability in action durations. This guarantees that counterfactual comparisons reflect genuine
 1919 causal differences, rather than artifacts of capturing frames at arbitrary, non-equivalent time indices.
 1920

1921 **F.2.5 SUMMARY.**

1922 Taken together, these design choices preserve consistency at both structural and temporal levels.
 1923 The ECS architecture ensures local mechanics map cleanly to modular causal mechanisms, while
 1924 the screenshot system anchors each player turn contrast to a canonical *impact frame* selected via
 1925 PoMA. By aligning contrasts at the most expressive phase of interaction, the system guarantees that
 1926 observed differences reflect genuine causal effects rather than timing artifacts, producing impact
 1927 frames that are both causally and semantically consistent.
 1928

1929 **G SPECIFICATIONS OF GENERATED VIDEO CLIPS**
 1930

1931 Generated video clips have following technical specifications:
 1932

1933 **G.1 RESOLUTION AND FORMAT**
 1934

1935 All video clips are rendered at a resolution of 512×512 pixels in a square aspect ratio. Videos are
 1936 encoded in MP4 format using the H.264 codec with `yuv420p` pixel format to ensure broad compati-
 1937 bility across video players and analysis frameworks.
 1938

1939 **G.2 FRAME RATE, DURATION, AND TIMING**
 1940

1941 Videos are captured at 50 frames per second (FPS) using a fixed-interval delta time method to ensure
 1942 consistent temporal sampling across all generated clips. This approach decouples game simulation
 1943 time from wall-clock time, enabling reproducible frame timing essential for dataset generation and
 comparative analysis.

1944 Video clip duration is variable and event-driven, spanning the complete battle sequence from initialization to completion. Clip length is determined by the termination of both player behavior trees, typically ranging from several seconds to longer sequences depending on the complexity of actions performed (e.g., melee attacks, spell casting, projectile interactions, defensive maneuvers).

1948

1949 G.3 DATASET ORGANIZATION

1950

1951 The system generates consistent contrasts, enabling direct comparison between observed battle outcomes and alternative scenarios under modified conditions. Each video file follows the naming convention `battle_XXXXXX-TIMESTAMP.mp4`, where `XXXXXX` represents a zero-padded 6-digit battle identifier. Accompanying JSON metadata files provide technical details including encoding parameters, frame timing information, and battle configuration data.

1955

1956 G.4 IMPLEMENTATION

1957

1958 Video generation utilizes the `imageio` library with PyAV backend for efficient encoding. The rendering pipeline captures frame sequences from the game’s screenshot buffer system, which also maintains temporal consistency in impact frames through the behavior tree execution framework.

1961

1962 G.5 VARIABLES GENERATED

1963

1964 In addition to clips, each generated example includes:

1965

- Controller inputs C_t
- Full or partial state X_t
- Mechanic-specific CL-DAG G^M
- Set of mechanic-specific parallel world DAGs
- Set of mechanic-specific counterfactual DAGs
- Seed / ω identifiers

1973

1974 H SUGGESTED METRICS

1975

1976

1977 Task	1978 Description	1979 Metric
1978 Fully observed mechanic inference	1979 Infer P_i using clips, game state variables, and controller inputs	$D_{KL}(P_i \parallel \hat{P}_i)$
1980 Partial (canonical) mechanic inference	1981 Infer P_i using clips and controller inputs, assuming game state is unobserved	$D_{KL}(P_i \parallel \hat{P}_i)$
1983 Generate consistent contrasts	1984 Generate multiple consistent contrast examples for each d_i associated with the mechanic, and validate that they are visually accurate and consistent	1985 Human or VLM validation
1986 Counterfactual abduction	1987 Generate $\{v_{X=x}, v_{X=x'}\}$ from game, obtain $\hat{v}_{X=x'} = \mathbb{E}[V_{X=x'} \mid V_{X=x} = v_{X=x}]$ using the model, then compare $\hat{v}_{X=x'}$ to $v_{X=x'}$	1988 Human or VLM validation

1989

1990

1991

Table 5: Tasks that can be used to evaluate mechanic learning with *Multiverse Mechanica*.

1992

1993

1994

1995

1996

1997

H.1 MECHANIC INFERENCE.

The fully- and partially-observed inference tasks require estimating the distributions \hat{P}_i implied by mechanic-specific constraints M and comparing them against the ground truth distributions P_i . We

1998 adopt KL-divergence as the primary quantitative measure, explicitly reporting $D_{\text{KL}}(P_i \parallel \hat{P}_i)$ for
 1999 each mechanic. This aligns with classical practice in distributional evaluation, where divergence to
 2000 the ground truth provides a direct measure of whether the model has captured the stochastic relations
 2001 induced by the mechanic.

2002 H.2 CONSISTENCY IN CONTRAST GENERATION.

2003 The contrast-generation and counterfactual-abduction tasks require evaluating whether pairs of clips
 2004 ($v_{X=x}, v_{X=x'}$) are *consistent*, i.e. differing only in outcomes attributable to the intervention variable
 2005 X while holding non-descendant factors fixed. Prior work has typically relied on human evaluation:
 2006 for example, Gingerson et al. (2024) collected large-scale human judgments of whether generated
 2007 gameplay videos adhered to intended mechanics. Recent work has investigated whether VLMs
 2008 can serve as automated evaluators of model generations. Hendriksen et al. (2025) show that pre-
 2009 trained VLMs can be adapted for evaluating world model rollouts, e.g. scoring whether predicted
 2010 videos match textual descriptions of target outcomes. However, to our knowledge, no prior work
 2011 has specifically used VLMs to evaluate *consistency* across parallel-world contrasts, as defined by
 2012 causal counterfactual principles. This remains an open direction, and *Multiverse Mechanica* pro-
 2013 vides level-3 parallel-world data where such evaluations can be systematically explored.

2014 Work by Monteiro et al. (2023) introduced *composition* metrics that effectively evaluate consistency
 2015 in image-based counterfactuals by checking whether attributes remain unchanged under controlled
 2016 edits. These metrics capture aspects of counterfactual faithfulness that parallel our notion of consis-
 2017 tency. However, they have not yet been extended to video data, nor applied to generative modeling of
 2018 game mechanics. We view *Multiverse Mechanica* as a platform to develop such extensions, allowing
 2019 both human and VLM-based evaluation methods to be compared side-by-side.

2020 H.3 SUMMARY.

2021 In short, our metrics combine classical distributional divergences for inference tasks with human-
 2022 or VLM-based consistency checks for contrastive generation tasks. This dual approach ensures that
 2023 models are evaluated not only on reproducing distributions of state variables but also on capturing
 2024 the causal consistency of gameplay dynamics under controlled interventions.

2025 I THEORETICAL AND IMPLEMENTATION DETAILS FOR PROOF-OF-CONCEPT

2026 I.1 BACKGROUND ON DIFFUSION MODELS AND REVERSE-SAMPLING

2027 Denoising diffusion probabilistic models (DDPMs) define a forward Markov chain that gradually
 2028 adds Gaussian noise to an image and a learned reverse process that denoises it step by step. Given
 2029 a data sample $x_0 \sim q(x_0)$, the forward process produces x_t by directly adding noise to the data:
 $2030 q(x_t|x_{t-1}) = \mathcal{N}(x_t; \sqrt{\alpha_t}x_{t-1}, (1 - \alpha_t)I)$ for $t = 1, \dots, T$. Here $0 < \alpha_t < 1$ are predefined
 2031 variances. In the reverse generation, one starts from pure noise $x_T \sim \mathcal{N}(0, I)$ and iteratively denoises to
 2032 x_0 using a model ϵ_θ trained to predict the injected noise. At each step, the model predicts $\hat{\epsilon} \approx \epsilon$ such
 2033 that x_{t-1} can be estimated by removing noise: e.g., $x_{t-1} = \frac{1}{\sqrt{\alpha_t}}(x_t - (1 - \alpha_t)\hat{\epsilon})$ (with additional
 2034 variance for stochastic sampling). In practice, one can also use the continuous-time formulation and
 2035 solve a reverse stochastic differential equation or its deterministic counterpart (as in DDIM), yielding
 2036 a mapping from an initial noise u directly to an image $x = G(u, c)$. Importantly, this exogenous
 2037 noise u acts as the stochastic latent that accounts for random variation in generated images. Using
 2038 a deterministic sampler (e.g., setting $\eta = 0$ in DDIM), one obtains a one-to-one mapping between u
 2039 and the output x , and can invert a given image to its corresponding u for a particular conditioning c .

2040 We will leverage this invertibility to extract the latent noise u_a from the original image x and the
 2041 latent noise u_b from the counterfactual image x_{cf} , where x denotes the factual image generated
 2042 under the original conditioning, x_{cf} represents the counterfactual image generated under modified
 2043 conditioning, u_a is the inverted latent noise corresponding to the factual image x , and u_b is the
 2044 inverted latent noise corresponding to the counterfactual image x_{cf} .

2052 I.2 BACKGROUND ON CAUSAL COUNTERFACTUALS IN IMAGE GENERATION
2053

2054 In causal terms, we can view the generative model as a structural causal model $x := f_\theta(u, c)$, where
2055 c is a cause (e.g., textual description or a set of discrete random variables) and u is an unobserved
2056 exogenous variable accounting for randomness. A counterfactual image aims to answer: “What
2057 would the image look like if we change c from c_A to c_B , while keeping all other latent factors
2058 the same?” The classical procedure for generating such counterfactuals is the three-step abduction-
2059 action-prediction: (1) Abduction: infer the exogenous noise u_a that produced the factual image x
2060 under c_A (this u_a captures the instance-specific variations of x); (2) Action: intervene by setting the
2061 prompt to c_B (while keeping u_a fixed); (3) Prediction: generate the new image as $x_{\text{cf}} = f_\theta(u_a, c_B)$.
2062 This procedure, if the model perfectly captures the true causal mechanism, would change only the
2063 aspects of the image directly affected by c and leave other details intact (satisfying causal consistency
2064 that no non-descendant features of c change). In practice, directly using u_a with a new prompt c_B
2065 can produce a reasonable edited image, but it may fail or produce artifacts if c_B demands alterations
2066 that conflict with the original latent factors.

2067 By contrast, many non-SCM image editing approaches do not explicitly enforce the same latent
2068 noise. For example, one might simply prompt the model with c_B and generate a new sample (dif-
2069 ferent u), or apply heuristics like latent interpolation, attention refocusing, or mask-based noising of
2070 only certain regions. These approaches can produce plausible results, but often lack guarantees that
2071 only the intended changes occur—the model might inadvertently change unrelated details because
2072 the random draw u or other generation conditions differ. Our goal is to incorporate causal prin-
2073 ciples into the diffusion editing process to maximize counterfactual faithfulness (only c -dependent
2074 changes) while still allowing the model flexibility to implement the edit realistically.

2075 I.3 CONTRASTIVE TRAINING VIA ALIGNMENT LOSSES
2076

2077 In this section, we provide the necessary background to help understand our method.

2079 I.4 NOTATION
2080

2081 We first define the notation used in our counterfactual editing framework. Let x denote the original
2082 (factual) image, and let x_{cf} denote the counterfactual image we aim to generate (the edited image
2083 after an intervention). We model image generation via a diffusion model as $x = G(u, c)$, where
2084 u is an initial exogenous noise (drawn from a Gaussian prior, typically $u \sim \mathcal{N}(0, I)$) and c is
2085 the conditioning (in our case, a text prompt). We use c_A for the original prompt and c_B for the
2086 counterfactual prompt. Using an inversion technique (e.g., reverse ODE or deterministic DDIM
2087 inversion), we can obtain u_a as the noise that generates x under c_A , and similarly u_b as the noise
2088 corresponding to x_{cf} under c_B . We denote by x_t the (noisy) latent image at diffusion timestep t when
2089 evolving toward x (with $x_0 = x$ and $x_T = u_a$ for the forward noising process), and likewise $x_{\text{cf},t}$ for
2090 the counterfactual trajectory. The diffusion model’s denoiser is denoted $\epsilon_\theta(x_t, c, t)$, which predicts
2091 the added noise at step t for latent x_t and conditioning c . For brevity, we write $\epsilon(x_t, c, t)$ when θ is
2092 clear from context. Finally, \mathcal{L}_1 , \mathcal{L}_2 , $\mathcal{L}_{\text{text}}$, and \mathcal{L}_{sub} will denote different loss terms introduced below.

2093 I.5 METHOD 1: L_1 – CONSISTENCY ALIGNMENT
2094

2095 Our first new loss function enforces consistency alignment between the factual and counterfactual
2096 generations. We obtain the noise u_a and u_b corresponding to x and x_{cf} respectively (via the inversion
2097 process described above). The consistency alignment loss is then defined as,

$$2099 \mathcal{L}_1 = \|u_a - u_b\|_2^2, \quad u_* = H_\theta^{T \leftarrow 0}(x_*, c_*) \quad (5)$$

2100 where $H_\theta^{T \leftarrow 0}$ represents the inversion function that maps from image space back to noise space at
2101 timestep T .

2102 Given the diffusion model $x = f_\theta(u, c)$, we have:

$$2104 x = f_\theta(u_a, c_A) \quad (6)$$

$$2105 x_{\text{cf}} = f_\theta(u_b, c_B) \quad (7)$$

2106 The inversion takes the image back to the noise, which yields:
 2107

$$u_a = H_\theta^{T \leftarrow 0}(x, c_A) \quad (8)$$

$$u_b = H_\theta^{T \leftarrow 0}(x_{\text{cf}}, c_B) \quad (9)$$

2111 The \mathcal{L}_1 is added to the training loss as a regularization term to enforce *exogenous invariance*. In
 2112 the ideal case where $u_b = u_a$, the counterfactual generation becomes:
 2113

$$x_{\text{cf}} = f_\theta(u_a, c_B) \quad (10)$$

2115 which ensures that all variations between x and x_{cf} are attributed solely to the conditioning change
 2116 $c_A \rightarrow c_B$, while preserving the exogenous factors encoded in u_a .
 2117

2118 This loss directly penalizes any differences between the underlying noise vectors of the original
 2119 and edited image. The motivation is to ensure that x and x_{cf} share the same source of variation, so
 2120 that as much of the scene’s random details as possible remain unchanged. This approach extracts
 2121 editing-related information from the seed, enabling differences to be more expressed by the condi-
 2122 tioning c rather than random variations. The primary change affects the reverse mapping/generator’s
 2123 decomposition of conditions, belonging to “seed-level” invariance.
 2124

2125 Intuitively, if u_a and u_b are identical, the only differences between x_{cf} and x will come from the
 2126 changed conditioning c_B vs c_A . In the ideal case, $\mathcal{L}_1 = 0$ means we are generating the counterfac-
 2127 tional with the exact same “random seed” as the factual image (the pure SCM counterfactual). This
 2128 encourages maximal consistency: the background, lighting, style, and other incidental attributes
 2129 should stay the same unless the new prompt explicitly demands their change. Enforcing \mathcal{L}_1 provides
 2130 strong alignment that leads to stable edits. It prevents the edited image from drifting in appearance
 2131 or composition: the counterfactual will tend to have the same objects and layout as the original,
 2132 only differing in the aspects dictated by the prompt change. This is beneficial for preserving identi-
 2133 ty (e.g., the same person’s face before and after an edit) and ensuring only the intended attributes
 2134 change.
 2135

2136 However, this strict constraint can also have a few limitations. If the counterfactual prompt c_B is
 2137 significantly different from c_A , using exactly the same noise u_a might overly constrain the genera-
 2138 tion, resulting in artifacts or an incomplete edit. The model might struggle to reconcile u_a (which
 2139 was optimal for the original content) with the new prompt, leading to implausible images or failure
 2140 to fully achieve the desired change.
 2141

2142 I.6 METHOD 2: L_2 – STRUCTURE PRESERVATION AT HIGH-NOISE

2143 As a more relaxed alternative, we propose to align the diffusion model’s behavior for the two im-
 2144 ages at the high-noise stages of generation, rather than forcing the initial noises to be identical.
 2145 Concretely, let S be a set of diffusion time steps focusing on the high-noise region (e.g., the latter
 2146 half or last third of the diffusion schedule, when x_t is still highly noisy). We define the structure
 2147 preservation loss \mathcal{L}_2 as:
 2148

$$\mathcal{L}_2 = \sum_{t \in S} \|\epsilon_\theta(x_t, c_A, t) - \epsilon_\theta(x_{\text{cf},t}, c_B, t)\|_2. \quad (11)$$

2149 \mathcal{L}_2 measures the disparity between the model’s denoising predictions for the factual versus counter-
 2150 factual image trajectories, but only at very noisy states (where x_t is mostly noise). By penalizing
 2151 this difference, we encourage the denoiser’s reaction to the two inputs to be the same in the early
 2152 stages of generation. This effectively steers $x_{\text{cf},t}$ to evolve in a similar direction as x_t while the
 2153 image is still coarse and noisy, ensuring the two generation processes start out aligned in terms of
 2154 global structure. Importantly, \mathcal{L}_2 does not enforce that the latent noises x_t themselves are exactly
 2155 equal, only that the predicted noise residuals (or equivalently, the score vectors) are similar. This
 2156 distinction makes \mathcal{L}_2 a partial relaxation of the \mathcal{L}_1 constraint. It nudges the counterfactual to have a
 2157 similar high-level appearance without locking in all the exact stochastic details.
 2158

2159 When using \mathcal{L}_2 , the model is free to adjust u_b as needed, but it will still preserve large-scale aspects
 2160 of u_a . For example, if x depicts a particular scene layout, \mathcal{L}_2 will bias x_{cf} to keep that layout,
 2161 since early denoising steps (which shape the overall composition) will be similar for both. As t
 2162 gets smaller (less noise), x_{cf} can gradually diverge more to realize the new content c_B specifies.
 2163

This approach maintains structure and identity better than an unconstrained edit, while granting more flexibility than L_1 for the model to incorporate the new prompt. In essence, L_2 focuses on aligning the coarse-grained features (which are determined in high-noise stages) and lets the fine details emerge freely.

One might consider applying a spatial mask so that structure preservation is enforced only on certain regions (for instance, only aligning the background areas that should remain unchanged). In our approach, we generally did not require an explicit mask for L_2 . Since L_2 operates on high-noise (low-detail) states, it inherently affects global structure more than specific fine features. We found that a well-balanced L_2 encourages overall consistency without needing per-pixel restrictions—the model naturally preserves unedited parts of the image. However, if a particular application demands strict locality (e.g., editing only a small region while leaving everything else exactly as is), a mask could be introduced to further ensure no influence of L_2 on the region to be changed (or conversely, to focus L_2 only on the region to preserve). In summary, L_2 already provides a soft, global consistency constraint, and masking is an optional refinement rather than a necessity in most cases.

I.7 ABDUCTION–ACTION–PREDICTION AND ITS DIFFUSION EMULATION

I.7.1 SCM SETUP.

Let $\mathcal{M} = (\mathbf{U}, \mathbf{V}, \mathbf{F}, P(\mathbf{U}))$ be a structural causal model with exogenous variables \mathbf{U} , endogenous variables \mathbf{V} , structural assignments \mathbf{F} , and exogenous distribution $P(\mathbf{U})$ (Pearl, 2009). We single out: (i) the *mechanic variables* $X \subseteq \mathbf{V}$ that we will intervene on; (ii) the *controller input* C ; and (iii) the visual variable V whose realization is a impact frame snapshot v . Throughout, we explicitly treat our generation seed ω as a realization of the SCM exogenous variables, i.e., $\omega \sim P(\mathbf{U})$, and we treat all other shared rendering conditions as part of ω (while C is held fixed explicitly).

I.7.2 ABDUCTION–ACTION–PREDICTION (AAP).

Given a factual observation v_0 obtained under $(X=x_0, C=c)$, the AAP recipe for the two-world case proceeds as:

- (**Abduction**) Infer $P(\mathbf{U} \mid V=v_0, X=x_0, C=c)$, choose a representative $\hat{\omega}$.
- (**Action**) Form the intervened model $\mathcal{M}_{X=x_1}$ while keeping $C=c$ and $\mathbf{U}=\hat{\omega}$ fixed.
- (**Prediction**) Evaluate the counterfactual $V_{X=x_1}(\hat{\omega})$.

Equivalently, in distributional form,

$$\hat{v}_1 \sim P(V_1 \mid V_0=v_0, X_0=x_0, C=c),$$

which is shorthand for propagating $\hat{\omega} \sim P(\mathbf{U} \mid V_0=v_0, X_0=x_0, C=c)$ through $\mathcal{M}_{X=x_1}$.

Algorithm 1 Abduction–Action–Prediction (two-world case)

Require: SCM $\mathcal{M} = (\mathbf{U}, \mathbf{V}, \mathbf{F}, P(\mathbf{U}))$, factual (v_0, x_0, c) , target x_1

- 1: **Abduction:** Infer $\hat{\omega} \leftarrow \text{MAP/mean/sample from } P(\mathbf{U} \mid V=v_0, X=x_0, C=c)$
- 2: **Action:** Construct $\mathcal{M}_{X=x_1}$; hold $C=c$ and $\mathbf{U}=\hat{\omega}$
- 3: **Prediction:** Compute $\hat{v}_1 \leftarrow V_{X=x_1}(\hat{\omega})$
- 4: **return** \hat{v}_1

I.8 DIFFUSION-BASED EMULATION OF AAP

In our latent diffusion setting, we emulate abduction–action–prediction (AAP) by identifying the SCM exogenous variables with the model’s initial latent noise:

$$\mathbf{U} \longleftrightarrow \omega \sim \mathcal{N}(0, I).$$

Abduction (DDIM inversion). We estimate $\hat{\omega}$ from a factual impact frame $V_{X=x_0}$ under (x_0, c) via deterministic sampler inversion (DDIM, $\eta=0$). Let $Z_{t,X=x_0}$ denote its noisy latents across

2214 $t \in [0, T]$. At each step, the denoiser $\epsilon_\theta(Z_{t, X=x_0}, t, c_0)$ predicts the noise, and inversion equations
 2215 (Appendix I.10.5) are used to propagate forward in the schedule, yielding an estimate $\hat{\omega} =$
 2216 $\text{Abduct}_\theta(Z_{0, X=x_0}, c_0)$.

2217 **Action.** Hold c fixed and change the mechanic state from x_0 to x_1 .

2219 **Prediction (deterministic reverse).** Initialize the trajectory with $Z_{T, X=x_1} := \hat{\omega}$ and run the de-
 2220 terministic reverse process conditioned on (x_1, c) to obtain a counterfactual latent $Z_{0, X=x_1}$, then
 2221 decode it to the counterfactual impact frame $\hat{V}_{X=x_1}$.

2223 **Algorithm 2** Diffusion-based AAP via DDIM ($\eta=0$)

2224 **Require:** Diffusion model $(\epsilon_\theta, \text{scheduler}, \text{decoder})$, factual $(V_{X=x_0}, x_0, c)$, target x_1
 2225 1: **Abduction:** $\hat{\omega} \leftarrow \text{Abduct}_\theta(Z_{0, X=x_0}, c_0)$ // DDIM inversion in latent space
 2226 2: **Action:** Keep c fixed, set $X := x_1$
 2227 3: **Prediction:** $Z_{T, X=x_1} := \hat{\omega}$; for $t = T, \dots, 1$: $Z_{t-1, X=x_1} \leftarrow \text{DDIMStep}(Z_{t, X=x_1}, t, x_1, c; \epsilon_\theta)$;
 2228 $\hat{V}_{X=x_1} \leftarrow \text{decoder}(Z_{0, X=x_1})$
 2229 4: **return** $\hat{V}_{X=x_1}$

2231

2232 **I.8.1 CONNECTION TO OUR TRAINING LOSSES.**

2234 The AAP framing clarifies the roles of our loss components. (i) *Exogenous alignment* \mathcal{L}_1 encourages
 2235 shared-seed invariance by driving

$$2236 \text{Abduct}_\theta(Z_{0, X=x_0}, c_0) \approx \text{Abduct}_\theta(Z_{0, X=x_1}, c_1),$$

2238 for elements of the same contrast that share the true ω . This ensures the abduction step produces
 2239 consistent seeds across worlds. (ii) *Structure preservation* \mathcal{L}_2 aligns denoiser outputs $\epsilon_\theta(Z_{t, X=x_j}, t, c_j)$
 2240 at high-noise steps $t \in S$, enforcing agreement on coarse global structure during the early reverse
 2241 process. This mirrors AAP’s assumption that exogenous factors (ω) are held fixed while only X
 2242 changes.

2243

2244 **I.8.2 SCM \leftrightarrow DIFFUSION MAPPING (TWO-WORLD CASE).**

2245

2246 SCM concept	2247 Diffusion instantiation
2248 Exogenous \mathbf{U}	\leftrightarrow Initial latent noise seed $\omega \sim \mathcal{N}(0, I)$
2249 Abduction $P(\mathbf{U} \mid V_{X=x_0}, x_0, c)$	\leftrightarrow DDIM ($\eta=0$) latent inversion $\hat{\omega} = \text{Abduct}_\theta(Z_{0, X=x_0}, c_0)$
2250 Action $X = x_1$	\leftrightarrow Condition reverse process on (x_1, c)
2251 Prediction $V_{X=x_1}(\hat{\omega})$	\leftrightarrow Deterministic reverse to $Z_{0, X=x_1}$ then decode $\hat{V}_{X=x_1}$
2252 Causal consistency	\leftrightarrow Shared seed $\hat{\omega}$; early-step structure preservation (\mathcal{L}_2)

2253

2254 Abduction via DDIM inversion yields an *estimate* $\hat{\omega}$ whose fidelity depends on the schedule and
 2255 conditioning; see Appendix I.10.6 for caveats and tuning guidance.

2256

2257 **I.9 ADDITIONAL REGULARIZERS**

2258 Beyond the core losses L_1 and L_2 , our framework can incorporate additional terms to improve
 2259 consistency and fidelity:

2261

2262 **I.9.1 SUBSPACE CONSISTENCY LOSS.**

2263 We can encourage the factual and counterfactual images to remain close in certain intermediate rep-
 2264 resentations of the diffusion model. For example, one may align hidden latents or cross-attention
 2265 maps at corresponding diffusion steps. By penalizing differences in these subspaces (e.g., the
 2266 model’s multi-head attention maps for background tokens, or feature maps in a particular UNet
 2267 layer), we enforce that the internal generation pathways for x and x_{cf} stay similar. This helps pre-
 2268 serve layout and identity at a semantic level, complementing the pixel-space alignment enforced by

L_1/L_2 . Formally, if $F_t(x)$ denotes some feature (such as a latent embedding or attention tensor) computed during the denoising of x at step t , we can define a loss $L_{\text{sub}} = \sum_{t \in \mathcal{T}} \|F_t(x) - F_t(x_{\text{cf}})\|_2$ for some chosen set of layers or timesteps \mathcal{T} . This subspace consistency loss encourages the edited image to differ only minimally in features unrelated to the intervention.

Text Consistency Loss. To ensure the edited image indeed reflects the counterfactual prompt c_B , we include a text-image consistency term. We rely on a pretrained image-text similarity model (such as CLIP) to measure alignment between x_{cf} and the description c_B . Let $\text{sim}(x_{\text{cf}}, c_B)$ be a similarity score (higher means the image matches the prompt better). We define a loss $L_{\text{text}} = -\text{sim}(x_{\text{cf}}, c_B)$ (or equivalently $1 - \text{sim}$, depending on the normalization) so that minimizing L_{text} maximizes the agreement between the generated image and the desired attributes. This ensures that while preserving content, we do not under-shoot the edit: the new image should clearly exhibit the prompted change. The text consistency loss guides the generation to remain faithful to the user’s request, especially when L_1 or L_2 are pulling towards the original image. It helps avoid the outcome where the edit is so conservative that the difference between x_{cf} and x is hard to discern.

I.10 LOSS COMBINATION

Our full counterfactual editing objective combines these components in a weighted sum:

$$L_{\text{total}} = \lambda_1 L_1 + \lambda_2 L_2 + \lambda_3 L_{\text{text}} + \lambda_4 L_{\text{sub}}, \quad (12)$$

where λ_i are tunable weights that control the influence of each loss term. In practice, we choose these weights to balance identity preservation against effective editing. Typical values and trade-offs are as follows:

λ_1 (Consistency Alignment): This is often kept relatively small (e.g., λ_1 in the range 0 to 0.5) unless the edit is very minor. A small λ_1 nudges the initial noise vectors closer without forcing identity completely. Increasing λ_1 leads to more literal counterfactuals (very high consistency with the original image’s details), but if set too high it may prevent the new attributes from appearing strongly. There is a trade-off between maintaining background/identity (higher λ_1 favors this) and allowing change (lower λ_1 gives more freedom).

λ_2 (Structure Preservation): We usually give L_2 a moderate to high weight (on the order of 1.0) as it is the principal mechanism to preserve structure. λ_2 in a range roughly 0.5 to 2.0 works well. A larger λ_2 tightly constrains the high-level layout and style to match the original, which is good for identity preservation; however, if λ_2 is excessively large, it can act almost as strictly as L_1 , potentially impeding necessary changes. Reducing λ_2 allows the counterfactual generation to deviate more in composition if needed, but too low λ_2 might result in unwanted alterations in background or other objects.

λ_3 (Text Consistency): This weight should be high enough to ensure the edit actually happens (especially for subtle changes), but not so high that it overrides the preservation losses. In practice λ_3 is often set around 0.5 to 1.0 (assuming similarity is scaled to a comparable range) so that the image aligns with the prompt without artifacts. If λ_3 is set too low, the edit might be too conservative (the model might simply regenerate the original image to satisfy L_1/L_2). If λ_3 is too high, the model may introduce exaggerated or incorrect features to satisfy the prompt, possibly compromising identity or visual quality.

λ_4 (Subspace Consistency): If used, this is typically a small auxiliary weight (e.g., 0.1). Since L_{sub} operates on internal features, it can strongly bind the generation if overweighted. A modest λ_4 helps reinforce structural consistency without conflicting with the primary losses. Tuning λ_4 involves checking that it indeed improves preservation of details like face identity or scene layout, without, for example, freezing the image in an early-state that ignores the new prompt. In some cases, we might set $\lambda_4 = 0$ (i.e., not use this term) if we find L_1 and L_2 are sufficient; when used, it serves as an extra regularizer.

In summary, L_1 and L_2 provide a spectrum between strict and loose alignment, λ_3 drives the fidelity to the requested counterfactual change, and λ_4 can bolster consistency on a feature level. We recommend starting with a balanced combination (for instance, $\lambda_1 = 0.2, \lambda_2 = 1.0, \lambda_3 = 0.5, \lambda_4 = 0.1$).



(a) Factual: A 1-on-1 battle. Foe 1 type is archer, element is fire, weapon is bow, weapon element is none, has shield is false, action is shoot. Foe 2 type is warrior, element is fire, weapon is long sword, weapon element is none, has shield is false, action is idle. Foe turn is foe 1.

(b) Counterfactual: A 1-on-1 battle. Foe 1 type is warrior, element is fire, weapon is long sword, weapon element is none, has shield is false, action is idle. Foe 2 type is warrior, element is fire, weapon is long sword, weapon element is none, has shield is false, action is idle. Foe turn is foe 1.

Figure 14: Example counterfactual image pairs generated from finetuned text-to-image diffusion model.

I.10.1 DIFFUSION BACKBONE.

We use a pretrained Stable Diffusion variant with a deterministic sampler¹, which makes the mapping between exogenous noise u and image v approximately invertible. This enables abduction of u from an image and consistent reuse across parallel worlds. Classifier-free guidance is applied with scale 7.5, and the scheduler uses $T = 50$ steps.

I.10.2 CONDITIONING.

In the main text we describe conditioning directly on game state variables (e.g., shield, weapon type, block outcome). For implementation, these variables and outcomes are converted into natural-language captions for compatibility with CLIP text encoders. This is a nuisance parameterization: the underlying conditioning remains the game state variables.

I.10.3 TRAINING SETUP.

We fine-tune the network backbone (UNet) only, keeping the VAE and text encoder frozen. Batch size is 4, training runs for 50 epochs, with a cosine learning-rate schedule, weight decay 0.01, and gradient clipping. Images are peak-action snapshots extracted at canonical times in each episode to minimize temporal ambiguity.

I.10.4 ALIGNMENT LOSSES.

We mainly use two loss functions for finetuning:

- \mathcal{L}_1 : consistency alignment. After inverting both factual and counterfactual images to latent noise (u_a, u_b) , we penalize $\|u_a - u_b\|^2$, enforcing invariance of exogenous factors. Note that this loss function is very expensive due to it needs to inverse two sampling pathes for each counterfactual data pair. In practice, we only apply \mathcal{L}_1 to one data point per batch of training data.

¹specifically we use DDIM $\eta = 0$, also the deterministic samplers in Karras et al. (2022)

2376 • \mathcal{L}_2 : structure preservation at high noisy region (large SNRs). At early diffusion timesteps,
 2377 we penalize discrepancies between denoiser predictions for factual vs. counterfactual tra-
 2378 jectories, encouraging global structural consistency.
 2379

2380 Both terms can be weighted with coefficients λ_1, λ_2 .
 2381

2382 I.10.5 SEED ABDUCTION WITH DETERMINISTIC DIFFUSION.

2383 Our multiverse alignment objective requires that consistent contrasts share the same exogenous
 2384 noise ω . In deterministic samplers (e.g., DDIM), this means that two parallel reverse processes
 2385 ($Z_{t,X=x_0}$) $_{t=0}^T$ and ($Z_{t,X=x_1}$) $_{t=0}^T$ can be initialized with the same ω , ensuring non-descendant
 2386 content is consistent.
 2387

2388 Given an observed impact frame $V_{X=x}$ with controller input c , let $Z_{0,X=x}$ denote its clean latent
 2389 before decoding and $Z_{t,X=x}$ the noisy latent at step t . At each step, the denoiser $\epsilon_\theta(\cdot)$ predicts noise
 2390 $\epsilon_\theta(Z_{t,X=x}, t, c)$, which is then used to trace the trajectory backward through the noise schedule.
 2391 Iterating these updates recovers an estimate $\hat{\omega} = \text{Abduct}_\theta(V_{X=x}, c)$.
 2392

2393 Applying this inversion procedure to both members of a contrast yields $\hat{\omega}_{x_0}$ and $\hat{\omega}_{x_1}$, which ideally
 2394 coincide. The seed-consistency loss \mathcal{L}_1 penalizes their distance, providing a concrete operational-
 2395 ization of the causal consistency principle within deterministic diffusion.
 2396

I.10.6 CAVEATS.

2397 **Deterministic inversion.** We use DDIM with $\eta = 0$ for Abduct_θ , yielding an approximately bijec-
 2398 tive mapping between seed and latent trajectory under fixed conditioning and schedule. In practice,
 2399 invertibility is approximate and sensitive to: (i) the precise noise schedule; (ii) classifier-free guid-
 2400 ance settings; and (iii) conditioning (x, c) . Hence $\hat{\omega}$ should be treated as a consistent *estimate* rather
 2401 than a ground-truth latent.
 2402

I.10.7 CHOOSING THE HIGH-NOISE SET S FOR \mathcal{L}_2 .

2403 We select S as either (i) the last k steps of the schedule (empirically $k \in [\frac{T}{3}, \frac{T}{2}]$), or (ii) all t with
 2404 $\text{SNR}(t) \leq \tau$ for a threshold τ . A weighted variant uses $w_t \propto \text{SNR}(t)^{-\gamma}$ and
 2405

$$2406 \mathcal{L}_2^w = \sum_t w_t \|\epsilon_\theta(z_{0,t}, t, x_0, c) - \epsilon_\theta(z_{1,t}, t, x_1, c)\|_2^2.$$

2407 Under mild conditions, aligning score predictions at high-noise is connected to alignment in data
 2408 space via Stein’s identity.
 2409

I.10.8 SCOPE.

2410 This is a feasibility study. We claim no pixel-level counterfactual identification and provide only
 2411 qualitative illustrations. Future work may extend this approach to video sequences and more com-
 2412 plex mechanics.
 2413

J SOFTWARE DEPENDENCIES

J.1 GAME ENGINE.

2414 The game itself is implemented in Pygame, a lightweight Python library for 2D graphics and in-
 2415 teraction. We chose Pygame because it enables rapid prototyping of turn-based combat mechanics,
 2416 frame-accurate rendering of impact frames, and reproducible control of random seeds, all within a
 2417 Python environment that integrates smoothly with machine learning workflows.
 2418

J.2 CAUSAL MODELING.

2419 To formalize and simulate the causal generative process underlying gameplay, we use the Pyro
 2420 probabilistic programming library (Bingham et al., 2019). Pyro provides the primitives required to
 2421

2430 implement SCMs consistent with the game’s causal DAG, including stochastic functions for exogenous
 2431 variables, deterministic assignments for endogenous variables, and intervention operators. This
 2432 allows us to align the game engine’s execution trace with an explicit causal model, and to sample
 2433 parallel-world contrasts in a principled manner.

2434

2435 J.3 REPRODUCIBILITY.

2436

2437 Both components are integrated in a unified Python codebase, ensuring that gameplay, causal mod-
 2438 eling, and data generation can be run deterministically from a single seed.

2439

2440 J.4 GRAPH LIBRARIES.

2441

2442 We generate mDAGs, parallel-world graphs and counterfactual graphs using the `Y0` library (Hoyt
 2443 et al., 2025).

2444

2445 J.5 GRAPH SERIALIZATION.

2446 All graphs are serialized as directed graphs in JSON using a node-link format. Nodes are repre-
 2447 sented as JSON objects with keys for the node identifier and attributes, while edges are represented
 2448 as objects with source and target identifiers and an edge type field. In the case of mDAGs and
 2449 parallel world graphs, exogenous nodes are marked with the attribute `"exogenous": true`.
 2450 For example, the above example of an mDAG with observed nodes $\{A, B, C\}$, one directed edge
 2451 $A \rightarrow B$, and one hyper-edge $\{B, C\}$, is converted to a CL-DAG and serialized as follows:

```

2452 {
2453   "nodes": [
2454     {"id": "A"},  

2455     {"id": "B"},  

2456     {"id": "C"},  

2457     {"id": "N_{B,C}", "exogenous": true}
2458   ],
2459   "links": [
2460     {"source": "A", "target": "B", "type": "directed"},  

2461     {"source": "N_{B,C}", "target": "B", "type": "directed"},  

2462     {"source": "N_{B,C}", "target": "C", "type": "directed"}
2463   ]
2464 }
```

2465
 2466
 2467
 2468
 2469
 2470
 2471
 2472
 2473
 2474
 2475
 2476
 2477
 2478
 2479
 2480
 2481
 2482
 2483